WILEY

RESEARCH ARTICLE | OPEN ACCESS

Molecular Ontology of the Nucleus of Solitary Tract

Silvia Gasparini[1] | Gislaine Almeida-Pereira[1] | Ana Sofia Peraza Munuzuri[1] | Jon M. Resch[2,3] | Joel C. Geerling[1,3]

[1]Department of Neurology, University of Iowa, Iowa City, Iowa, USA | [2]Department of Neuroscience and Pharmacology, University of Iowa, Iowa City, Iowa, USA | [3]Iowa Neuroscience Institute, University of Iowa, Iowa City, Iowa, USA

Correspondence: Joel C. Geerling (joel-geerling@uiowa.edu)

ABSTRACT

The nucleus of the solitary tract (NTS) receives visceral information and regulates appetitive, digestive, and cardiorespiratory systems. Within the NTS, diverse processes operate in parallel to sustain life, but our understanding of their cellular composition is incomplete. Here, we integrate histologic and transcriptomic analysis to identify and compare molecular features that distinguish neurons in this brain region. Most glutamatergic neurons in the NTS and area postrema co-express the transcription factors *Lmx1b* and *Phox2b*, except for a ventral band of neurons in the far-caudal NTS, which include the *Gcg*-expressing neurons that produce glucagon-like peptide 1 (GLP-1). GABAergic interneurons intermingle through the *Lmx1b+Phox2b* macropopulation, and dense clusters of GABAergic neurons surround the NTS. The *Lmx1b+Phox2b* macropopulation includes subpopulations with distinct distributions expressing *Grp*, *Hsd11b2, Npff*, *Pdyn*, *Pou3f1*, *Sctr*, *Th*, and other markers. These findings highlight *Lmx1b–Phox2b* co-expression as a common feature of glutamatergic neurons in the NTS and improve our understanding of the organization and distribution of neurons in this critical brain region.

1 | Introduction

The first site in the brain that receives visceral information is the nucleus of the solitary tract, commonly referred to by the abbreviation of its original Latin name, *nucleus tractus solitarii* (NTS). This interoceptive region of the dorsomedial medulla surrounds the solitary tract, which is a distinctive bundle of myelinated axons delivering viscerosensory inputs to diverse neurons in and around the NTS (Cutsforth-Gregory and Benarroch 2017). NTS neurons integrate these peripheral inputs with top–down input from a variety of other brain regions (Gasparini et al. 2020; Holt, Pomeranz, et al. 2019; van der Kooy et al. 1984; Whitehead, Bergula, and Holliday 2000) and send output to forebrain and brainstem regions that regulate affective, appetitive, cardiorespiratory, and neuroendocrine functions (Beckstead, Morse, and Norgren 1980; Geerling and Loewy 2006; Herbert, Moga, and

Saper 1990; Holt 2022; Loewy and Burton 1978; Quillet et al. 2023; Rinaman 2010; Ter Horst et al. 1989).

The general organization of NTS neurons has been studied in a variety of species, including cats (Loewy and Burton 1978), humans (McRitchie and Tork 1993), hamsters (Whitehead 1988), rats (Altschuler et al. 1989; Herbert, Moga, and Saper 1990; Kalia and Sullivan 1982), and mice (Ganchrow et al. 2014). Previous tracing studies identified a mosaic pattern of inputs, with separate visceral structures providing input to overlapping NTS subregions (Altschuler et al. 1989; Bassi et al. 2022; Contreras, Beckstead, and Norgren 1982; Hamilton and Norgren 1984; Kalia and Sullivan 1982). Separate visceral stimuli activate neurons in separate NTS subregions (Ran et al. 2022), and intermingled clusters of NTS neurons express diverse molecular markers (Ludwig et al. 2021; Riche, De Pommery, and Menetrey 1990; Zhang et al. 2021), but

our ability to distinguish which subpopulations control which specific functions remains limited.

One limiting factor is a lack of knowledge about the overall spatial and molecular organization of NTS neurons. Neurons with separate connections and functions can be distinguished by differences in gene expression, and using molecular-genetic features to distinguish neurons is a useful strategy in both humans and experimental animals (Siletti et al. 2023; Yao et al. 2023; Zeisel et al. 2018). For example, clarifying the molecular ontology of the parabrachial nucleus, which receives output from the NTS, revealed that intermingled populations of neurons have different connectivity patterns and functions (Karthik et al. 2022; Pauli et al. 2022). Clarifying the molecular ontology of the NTS could lay the foundation for linking specific neurons to their specific functions.

Transcription factors control gene expression, and the transcriptome of each neuron influences the pattern of synaptic connections it establishes (Hirsch et al. 2021). This property makes transcription factors particularly useful for identifying and distinguishing neurons in the hindbrain (Gray 2013; Karthik et al. 2022). Transcription factors with expression patterns that overlap the NTS include *Lmx1b*, which is important for the development of certain monoaminergic and glutamatergic neurons in the brainstem (Dai et al. 2008), and *Phox2b*, which is necessary for the development of specific catecholaminergic and glutamatergic populations, including the NTS (Dauger et al. 2003; Gray 2013; Kang et al. 2007). In this study, we combined histological analysis with publicly available transcriptomic data to investigate the spatial distributions of these two transcription factors and a variety of other molecular markers that identify and distinguish neuronal subpopulations in and around the NTS.

2 | Materials and Methods

2.1 | Mice

All mice were group-housed in a temperature- and humidity-controlled room on a 12/12 h light/dark cycle and with ad libitum access to water and standard rodent chow. Overall, we used $n = 40$ (31 males and 9 females) mice ranging in age from 8 to 16 weeks (20–40 g body weight). Included among these were knockin-Cre and Cre-reporter strains detailed in Table 1. These mice were hemizygous and maintained on a C57BL6/J background. All experiments were conducted in accordance with the guidelines of the Institutional Animal Care and Use Committee at the University of Iowa.

2.2 | Perfusion and Tissue Sections

Mice were anesthetized with a mixture of ketamine–xylazine (i.p. 150-15 mg/kg, dissolved in sterile 0.9% saline), then perfused transcardially with phosphate-buffered saline (PBS), followed by 10% formalin–PBS (SF100-20, Fisher Scientific). After perfusion, brains were removed and fixed overnight in 10% formalin–PBS. We sectioned each brain into 40-μm-thick coronal slices using a freezing microtome and collected tissue sections into sepa-

rate, one-in-three series. Sections were stored in cryoprotectant solution at −20°C until further processing.

2.3 | Immunofluorescence Labeling

For immunofluorescence labeling of mouse brain tissue, we removed from cryoprotectant 6–9 evenly spaced axial tissue sections from the caudal medulla for $n = 3$ cases for each marker combination. We rinsed all sections in PBS, then loaded them into a solution containing one or more primary antisera (Table 2). These antisera were added to a PBS solution of 0.25% Triton X-100 (BP151-500, Fisher), 2% normal donkey serum (NDS, 017-000-121, Jackson ImmunoResearch), and 0.05% sodium azide (14314, Alfa Aesar) as a preservative (PBT–NDS–azide). We incubated sections overnight at room temperature on a tissue shaker. The following morning, the sections were washed 3× in PBS and incubated for 2 h at room temperature in PBT–NDS–azide solution containing species-specific donkey secondary antibodies. These secondary antibodies were conjugated to Cy3, Cy5, Alexa Fluor 488, Brilliant Violet, or biotin (Jackson ImmunoResearch #s 703-545-155, 705-545-147, 705-165-147, 706-165-148, 706-065-148, 713-065-147, 711-165-152, 711-545-152, 711-675-152, 711-175-152, 715-545-003, 715-165-150, 715-065-151, 715-545-150; each diluted 1:1000 or 1:500). If a biotinylated secondary antibody was used, sections were again washed 3× in PBS, then incubated for an additional 2 h in streptavidin-Cy5 #SA1011; Invitrogen). Tissue sections were then washed 3× in PBS, mounted on glass slides (#2575-plus; Brain Research Laboratories), dried, and then coverslipped using Vectashield (Vector Labs). All slides were stored in slide folders at 4°C until imaging. For immunofluorescence labeling of the nuclear transcription factor Pou3f1 and the cytoplasmic enzyme neuronal nitric oxide synthase (nNOS), available antisera both were rabbit primaries. Thus, we incubated tissue in Pou3f1 antibody overnight, followed by 3× washes in PBS then Cy3-donkey-anti-rabbit for 2 h on the second day. Then, we washed the tissue in PBS and incubated it overnight in the nNOS primary antibody overnight, followed by 3× washes in PBS then Alexa Fluor 488-donkey-anti-rabbit secondary antibody for 2 h on the third day. This protocol allowed us to use both primaries made in the same host, labeling one protein in the nucleus and the other in the cytoplasm.

2.4 | Immunohistochemistry

For brightfield labeling of mouse brain tissue, we removed a full-brain series of tissue sections from cryoprotectant for $n = 3$ cases, rinsed them in PBS, then incubated them in 0.3% hydrogen peroxide (#H325-100, Fisher), in PBT for 30 min to quench endogenous peroxidase activity. After three washes in PBS, we loaded sections into PBT–NDS–azide containing one primary antiserum overnight at room temperature on a tissue shaker. After 3× PBS washes the following morning, we incubated sections for 2 h in a 1:500 solution of biotinylated specie-specific donkey antibody (#711-065-152; Jackson) in PBT–NDS–azide. Sections were washed three more times and placed for 1 h in biotin–avidin complex (Vectastain ABC kit PK-6100; Vector), washed 3× in PBS, and incubated in nickel–diaminobenzidine (NiDAB) solution for 10 min. Our stock DAB solution was prepared by adding 100 tablets (#D-4418, Sigma, Saint Louis, MO) into 200 mL ddH$_2$O, then filtering it. We then used 1 mL

TABLE 1 | Cre-driver and -reporter mice.

Strain	References	Source information	Key gene
R26-LSL-L10GFP Reporter	Krashes, M. J., B. P. Shah, J. C. Madara, et al. 2014. "An Excitatory Paraventricular Nucleus to AgRP Neuron Circuit That Drives Hunger." *Nature* 507, no. 7491: 238.	Available from originating investigators http://www.informatics.jax. org/allele/MGI:5559562	Floxed transcription STOP cassette followed by EGFP/Rpl10 fusion reporter gene under the control of the CAG promoter targeted to the Gt(ROSA)26Sor locus
Vgat-IRES-Cre (Slc32a1-IRES-Cre)	Vong, L., C. Ye, Z. Yang, B. Choi, S. Chua, B. B. Lowell. 2011. "Leptin Action on GABAergic Neurons Prevents Obesity and Reduces Inhibitory Tone to POMC Neurons." *Neuron* 71, no. 1: 142–154.	*Jax 028892* https://www.jax.org/strain/ 028862	*IRES-Cre inserted after the Slc32a1 stop codon*
Vglut2-IRES-Cre (Slc17a6-IRES-Cre)	Vong, L., C. Ye, Z. Yang, B. Choi, S. Chua, B. B. Lowell. 2011. "Leptin Action on GABAergic Neurons Prevents Obesity and Reduces Inhibitory Tone to POMC Neurons." *Neuron* 71, no. 1: 142–154.	*Jax 016963* https://www.jax.org/strain/ 016963	*IRES-Cre inserted downstream of the stop codon of Slc17a6 on chromosome 7*

TABLE 2 | Antisera used in this study.

Antigen	Immunogen description	Source, host species, RRID	Concentration
Choline acetyltransferase (ChAT)	Human placental choline acetyltransferase	Millipore, goat polyclonal, #AB144P; RRID: AB_2079751	1:1000
Green fluorescent protein (GFP)	Full length green fluorescent protein from the jellyfish *Aequorea Victoria*	Thermo Fisher Scientific, Chicken, #A10262; RRID: AB_2534023	1:3000
11-beta-hydroxysteroid dehydrogenase type 2 (HSD2)	Fusion protein Ag5146 (amino acids 1–405 encoded by human *HSD11B2*; GenBank BC036780)	Protein Tech, rabbit polyclonal, cat# 14192-1-AP; RRID: AB_2119643	1:2000
11-beta-hydroxysteroid dehydrogenase type 2 (HSD2)	Amino acids 261–405 from the C-terminus of human 11β-HSD2	Santa Cruz, rabbit polyclonal, cat# sc_20176; RRID: AB_2233199	1:700
Lmx1b	Full-length LIM homeobox transcription factor 1 beta protein from mouse	C. Birchmeier, Max Delbruck Center for Molecular Medicine, Berlin; guinea pig polyclonal, RRID: AB_2314752	1:8000
Neuronal nitric oxide synthase (nNOS)	A recombinant protein consisting of 195 amino acids from the N-terminus of rat nNOS protein	Invitrogen, Rb polyclonal, RRID:AB_2313734	1:1000
Paired-like homeobox 2b (Phox2b)	Mouse monoclonal antibody raised against amino acids 11–70 mapping near the N-terminus Phox2b of human origin	Santa Cruz mouse, monoclonal, # sc-376997, RRID: AB_2813765	1:1000
Paired-like homeobox 2b (Phox2b)	BSA-coupled 15mer corresponding to the C terminus of the Phox2b protein with an added N-terminal tyrosine	H. Enomoto, School of Medicine at Kobe University, Japan; RRID: AB_2895590	1:12,000
Oct6 (Pou3f1)	Synthetic peptide within human Oct6	Abcam, rabbit monoclonal: #ab126746; RRID: AB_11130256	1:2000
Tyrosine hydroxylase (TH)	Native tyrosine hydroxylase from rat pheochromocytoma in sheep host	Millipore, sheep polyclonal, cat#: Ab1542; RRID: AB_90755	1:2000

TABLE 3 | RNAscope probes used for fluorescence in situ hybridization.

Probe	Common name for target gene/mRNA	Channel	ACD catalog #	Lot #
Mm-Npff	Neuropeptide FF	C1	479901	20290A
Mm-Gcg-C3	Glucagon/Glucagon-like peptide-1	C3	400601-C3	24172E
Mm-Grp-C2	Gastrin-releasing peptide	C2	317861-C2	19211A
Mm-Pdyn-C3	Prodynorphin	C3	318771-C3	17290A
Mm-Phox2b-C2	Phox2b	C2	407861-C2	19179B
Mm-Sctr-C2	Secretin receptor	C2	508511	23163

of this DAB stock solution, with 300 µL of 8% nickel chloride (#N54-500, Fisher Chemical) per 6.5 mL PBS. After 10 min in NiDAB, we added hydrogen peroxide (0.8 µL of 30% H_2O_2 per 1 mL PBS-DAB) and swirled sections for 2–5 min until observing black (nickel–DAB) color change. After two rapid PBS washes, we wet-mounted one or more sections, checked them in a light microscope to ensure optimal staining, and in rare cases replaced sections for up to one additional minute for additional enzymatic staining. Finally, after washing an additional 3× in PBS, we ordered sections and mounted them on glass slides. Slides were air-dried then dehydrated in an ascending series of alcohols and xylenes, then coverslipped with Cytoseal 60 (#8310-16 Thermo Scientific).

2.5 | Fluorescence In Situ Hybridization

To label mRNA, we used a variety of different RNAscope probes, detailed in Table 3, along with the RNAscope Fluorescent Multiplex Reagent Kit (#320851; Advanced Cell Diagnostics) or RNAscope Fluorescent Multiplex Detection Kit v2 (#323100; Advanced Cell Diagnostics). To label tissue using the original Fluorescent Multiplex Reagent Kit, we first mounted a one-in-three series of brainstem tissue slices containing the NTS on glass slides, then left slides to dry overnight. Sections were outlined using a Super-HI PAP pen (Research Products Incorporated) to form a hydrophobic barrier, then we washed with PBS 2 × 2 min at room temperature. Then, we incubated the slices with Protease IV in glass petri dishes floating in a 40°C water bath for 30 min and washed with PBS 2 × 2 min. Next, we incubated sections in combinations of probes from Table 3 for 2 h at 40°C. After that, we incubated slides in AMP1-4-FL for 15–30 min each at 40°C and washed with RNAscope wash buffer (#320058; diluted 1:50 in ddH$_2$O) 2 × 2 min between steps.

To label tissues using the Multiplex Fluorescent Reagent Kit v2, we removed tissue from cryoprotectant, mounted them on glass slides, and allowed them to dry for 1 h, then washed with PBS for 5 min, baked for 30 min at 60°C, and then postfixed in 10% neutral buffered formalin (NBF) for 15 min at 4°C. Slides were then dehydrated in a series of 50% ethanol, 70% ethanol, and 100% ethanol solutions, for 5 min each. After repeating the 100% ethanol step, slides were allowed to dry at room temperature. Sections were incubated in hydrogen peroxide (#322380; Advanced Cell Diagnostics) for 10 min at room temperature, then washed with distilled water in two 2-min washes. We next outlined sections to form a hydrophobic barrier using an ImmEdge pen (Vector Laboratories). The slides were then covered with Protease III,

incubated for 30 min at 40°C, then washed for 2 min, twice using ultrapure water. The sections were then incubated in RNAscope probes (Table 2) for 2 h at 40°C. After that, AMPs 1−3 were added, in series, for 15−30 min each, at 40°C, with two 2-min rinses in 1× RNAscope Wash Buffer between each step. Sections were covered by channel-specific HRP for 15 min at 40°C, then 150−200 µL Opal dye (cat# FP1496001KT; Akoya Biosciences) for 30 min at 40°C, then HRP blocker for 15 min at 40°C, with two 2-min RNAscope Wash Buffer rinses between each step. After HRP, we either rinsed sections with PBS 2× or performed an immunofluorescence protocol to label HSD2 or L10GFP. For this, we incubated sections in a PBT–NDS–azide solution with a primary antiserum (either rabbit anti-HSD2 or chicken anti-GFP) overnight at 4°C. After washing 3× with PBS the next morning, we incubated sections at 4°C for an additional 2 h in a PBT–NDS–azide solution containing a fluorophore-conjugated secondary antibody (either Cy3-conjugated donkey anti-rabbit or Alexa Fluor 488-conjugated anti-chicken). After a final set of PBS washes, we coverslipped all slides using Vectashield with DAPI.

2.6 | Imaging, Analysis, and Figures

All slides were scanned using an Olympus VS120 microscope. We began by first acquiring a 2× overview scan and then using a 10× objective to scan all tissue sections. We then acquired 20× and in some cases 40× *z-stacks* encompassing all regions of interest for this study. For each slide, this produced a virtual slide image (VSI) file containing a 10× whole-slide layer, plus separate layers with 20× and/or 40× extended-focus images in regions of interest. For brightfield images of NiDAB cases immunolabeled for Phox2b or Lmx1b, we used a 20× objective with extended focal imaging (EFI) to collect and combine in-focus images from 15 focal planes through the tissue.

After reviewing data in OlyVIA (Olympus), we used cellSens to crop full-resolution images and Adobe Photoshop to adjust brightness and contrast. We used Adobe Illustrator to make drawings, plot cells for figures, arrange images, and add lettering for figure layouts. Scale bars were traced in Illustrator atop calibrated lines from cellSens to produce clean white or black lines in each figure.

2.7 | Nomenclature

For mouse genes, we used MGI nomenclature. For proteins and Cre-reporters, we used common abbreviations from the

published literature. For rostrocaudal levels and major subdivisions of the NTS in mice, we adapted the general schema conceived in rats by Saper and colleagues, who subdivided the NTS into three levels (rostral, intermediate, and caudal) and two subdivisions (medial and lateral; Herbert, Moga, and Saper 1990). For other neuroanatomical structures and cell populations, we used and referred to nomenclature defined in peer-reviewed neuroanatomical literature.

3 | Results

3.1 | Distinguishing NTS From Surrounding Neurons

Partly distinct distributions of neurons express the nuclear transcription factors *Phox2b* and *Lmx1b* (Dai et al. 2008; Kang et al. 2007), but plotting the adult distribution of NiDAB immunolabeling for each transcription factor revealed the NTS as a prominent region of overlap. In the dorsomedial medulla, a dense concentration of neurons expressing each transcription factor covered all subdivisions of the NTS at all rostrocaudal levels, as well as the area postrema (black arrows in Figure 1). In contrast, these two transcription factors identified largely separate neuronal distributions outside the NTS. For example, *Phox2b*-expressing neurons filled the dorsal vagal motor nucleus (DMV) and nucleus ambiguus (green arrows in Figure 1a–d), while *Lmx1b*-expressing neurons were prominent in the medullary raphe and spinal trigeminal nuclei (blue arrows in Figure 1e–h). Both transcription factors identified scattered neurons in the medullary reticular formation, rostral and ventrolateral to the NTS.

Immunofluorescence labeling confirmed the extensive *Phox2b* distribution in the NTS, area postrema, and DMV and revealed its nearly uniform co-localization with *Lmx1b* in neurons across the NTS and area postrema (Figure 2a–d), plus a small number of neurons extending through the ventrolateral margin of the NTS and into the reticular formation. Both *Phox2b* and *Lmx1b* were absent from the large, ChAT-immunoreactive somatomotor neurons of the hypoglossal nucleus (Figure 2a). Dorsal to the hypoglossal nucleus and immediately ventral to the NTS, we did not find any *Lmx1b* in DMV neurons, which contained nuclear immunoreactivity for *Phox2b* and cytoplasmic immunoreactivity for choline acetyltransferase (ChAT, blue in Figure 2e–g), nor was *Lmx1b* expressed in any *Phox2b*-expressing and ChAT-immunoreactive neurons of the nucleus ambiguus (not shown). Thus, co-expression of *Lmx1b* identifies a large, noncholinergic subset of *Phox2b*-expressing neurons in the NTS and area postrema.

3.2 | Fast-Neurotransmitter Phenotype of NTS Neurons

To determine the fast-neurotransmitter phenotype of *Lmx1b*-expressing NTS neurons and understand the overall proportions of NTS glutamatergic or GABAergic neurons expressing this transcription factor, we used Cre-reporter mice for the vesicular GABA transporter (*Slc32a1*/Vgat) or the vesicular glutamate transporter (*Slc17a6*/Vglut2). In *Slc32a1*/Vgat reporter mice, GABAergic neurons intermingled with *Lmx1b*-expressing neurons throughout the NTS and area postrema, but none expressed

Lmx1b (Figure 3a–c). GABAergic neurons also formed dense clusters in the parasolitarius nucleus (between the dorsal NTS and gracile nucleus) and in the ventrolateral NTS. In *Slc17a6*/Vglut2 reporter mice, a large majority of glutamatergic neurons in the NTS and area postrema expressed *Lmx1b* (Figure 3d–f).

3.3 | Some Caudal, Ventral Neurons Lack *Phox2b* and/or *Lmx1b*

Plotting neurons across successive rostrocaudal levels (Figure 4a–d) revealed a ventral band of glutamatergic neurons lacking *Lmx1b* in the far-caudal NTS (Figure 4d). Although some of these glutamatergic neurons did express *Phox2b*, many of them lacked both transcription factors (Figure 5). Thus, *Lmx1b* co-expression with *Phox2b* identifies a noncholinergic, glutamatergic majority of neurons in the NTS and area postrema, except for far-caudal, ventral neurons that express *Phox2b* alone (without *Lmx1b*), and an intermingled subset that lacks both transcription factors. Far-caudal neurons lacking both *Phox2b* and *Lmx1b* are larger, with horizontally elongated somata and dendrites, and their distribution extends laterally, into the reticular formation.

3.4 | Subpopulations of NTS Neurons

Next, we labeled markers for three well-established subpopulations of NTS neurons to clarify their relationships to the intersectional *Lmx1b*+*Phox2b* macropopulation of NTS glutamatergic neurons and to one another.

First, we immunolabeled the enzyme 11-beta-hydroxysteroid dehydrogenase type 2 (HSD2). This glucocorticoid-metabolic enzyme identifies a population of approximately 200 neurons that sense aldosterone and selectively increase sodium appetite (Gasparini et al. 2024, 2019; Jarvie and Palmiter 2017; Resch et al. 2017). Across the characteristic V-shaped distribution of HSD2-immunoreactive neurons, between the subpostremal NTS and the DMV, a large majority contained *Lmx1b* (Figure 6a,b), and all HSD2 neurons contained nuclear *Phox2b* immunoreactivity, as reported previously (Gasparini et al. 2019; Geerling, Chimenti, and Loewy 2008; Resch et al. 2017).

Second, we immunolabeled tyrosine hydroxylase (TH). This rate-limiting enzyme for catecholamine synthesis identifies multiple subsets of glutamatergic-catecholaminergic neurons in the NTS and area postrema (Stornetta, Sevigny, and Guyenet 2002; Zhang et al. 2021). TH-immunoreactivity was mutually exclusive with HSD2, and TH-immunoreactive neurons had a broader overall distribution in the NTS and area postrema (Figure 6). Many, small TH-immunoreactive neurons distributed through the area postrema and extended laterally and ventrally into the subpostremal NTS ("A2d" population). All of these smaller neurons contained intense nuclear immunoreactivity for *Lmx1b*. Further ventrally, larger and medium-sized TH-immunoreactive neurons clustered along the dorsolateral edge of the DMV ("A2" population) and extended into far-caudal levels of the NTS, behind the area postrema. This ventral subpopulation of larger TH-immunoreactive neurons had lighter and more variable *Lmx1b* expression, with some members in the far-caudal NTS lacking this transcription factor entirely. All TH-immunoreactive
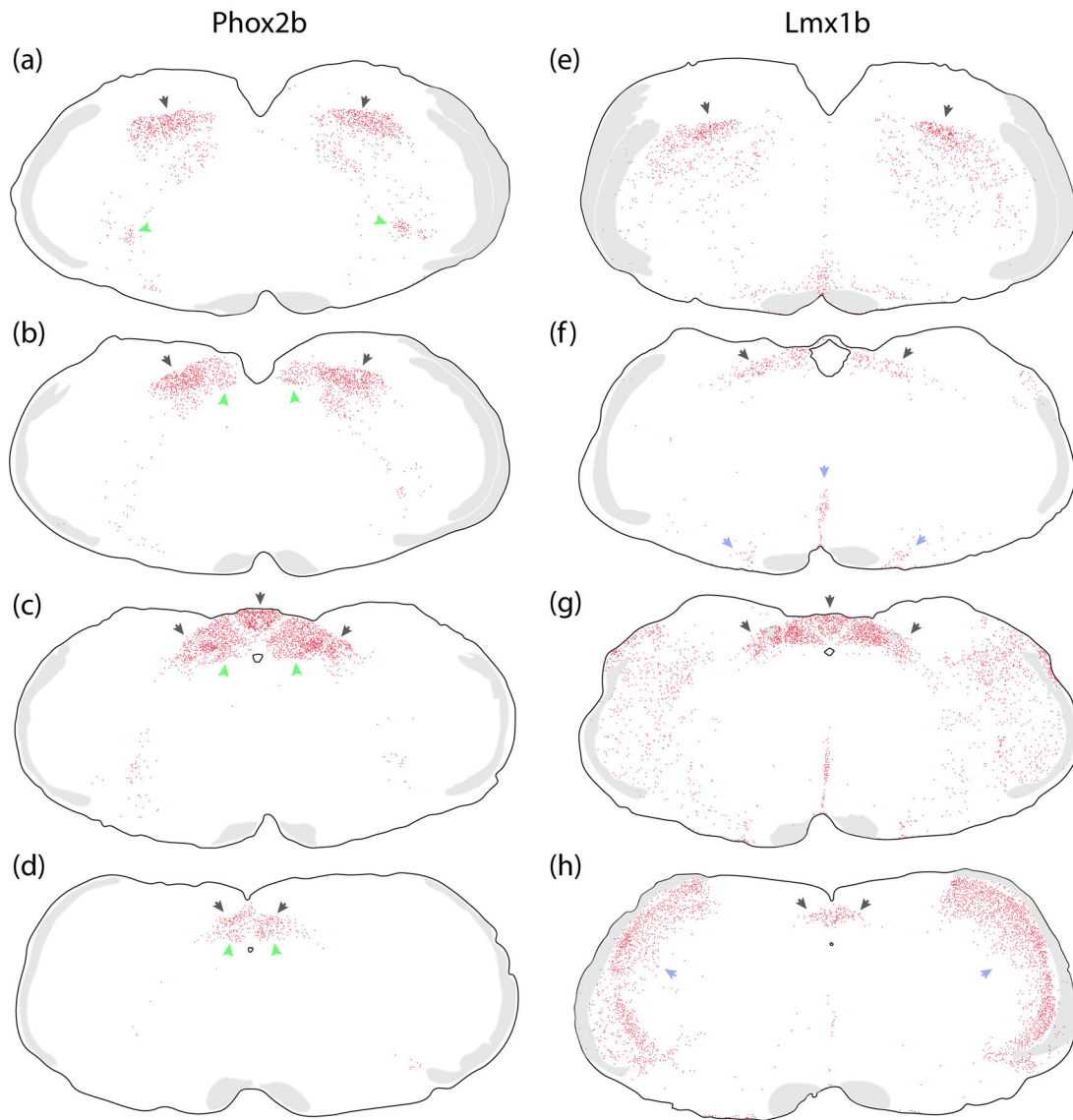
FIGURE 1 | Distribution of neurons expressing the transcription factors Phox2b (a–d) and Lmx1b (e–h) at four rostrocaudal levels of the mouse brainstem. Each red dot represents one neuron with nuclear immunolabeling. Black arrowheads highlight dense concentrations in the dorsomedial medulla, nucleus of the solitary tract (NTS), and area postrema. The green arrowheads highlight Phox2b-immunoreactive neurons in the nucleus ambiguus (a) and in the dorsal vagal motor nucleus (DMV, b–d). Blue arrowheads Lmx1b-immunoreactive neurons in the medullary raphe and parapyramidal nuclei (f) and in the outer layers of the spinal trigeminal nucleus (h).

neurons had strong nuclear immunoreactivity for *Phox2b* (not shown).

Third, we immunolabeled *Pou3f1*, a transcription factor reported to identify neurons in a subregion of the NTS receiving vagal mechanosensory input from the esophagus (Lowenstein et al. 2023). *Pou3f1* co-localized with a prominent subset of *Lmx1b*-immunoreactive neurons in the NTS (Figure 7). At and immediately rostral to the obex, this round, dense cluster contained nuclear immunoreactivity for *Pou3f1* and cytoplasmic immunoreactivity for nNOS (Figure 8), which is a marker for esophageal premotor neurons (Wiedner, Bao, and Altschuler 1995) that are located in a subregion referred to as the central NTS subnucleus and that send output to the rostral (esophageal) subregion of the nucleus ambiguus (Cunningham and Sawchenko 1989; Herbert, Moga, and Saper 1990). Outside this prominent cluster, we found

lighter and more variable *Pou3f1* in additional neurons distributed caudally through the medial NTS. None of these contained HSD2 (not shown) or TH (Figure 7).

3.5 | Publicly Available Transcriptomic Data

Next, we sought markers for additional subpopulations within the *Lmx1b+Phox2b* glutamatergic macropopulation by reviewing single-cell RNA sequencing (scRNA-seq) data in the Allen Brain Cell Atlas (ABCA; https://knowledge.brain-map.org/abcatlas). This publicly available dataset includes transcriptomic data from four million aggregate cells collected from adult mouse brains (Yao et al. 2023). Before seeking novel markers, we began by assessing the alignment between these transcriptomic data and the core ontology of molecular markers shown above.
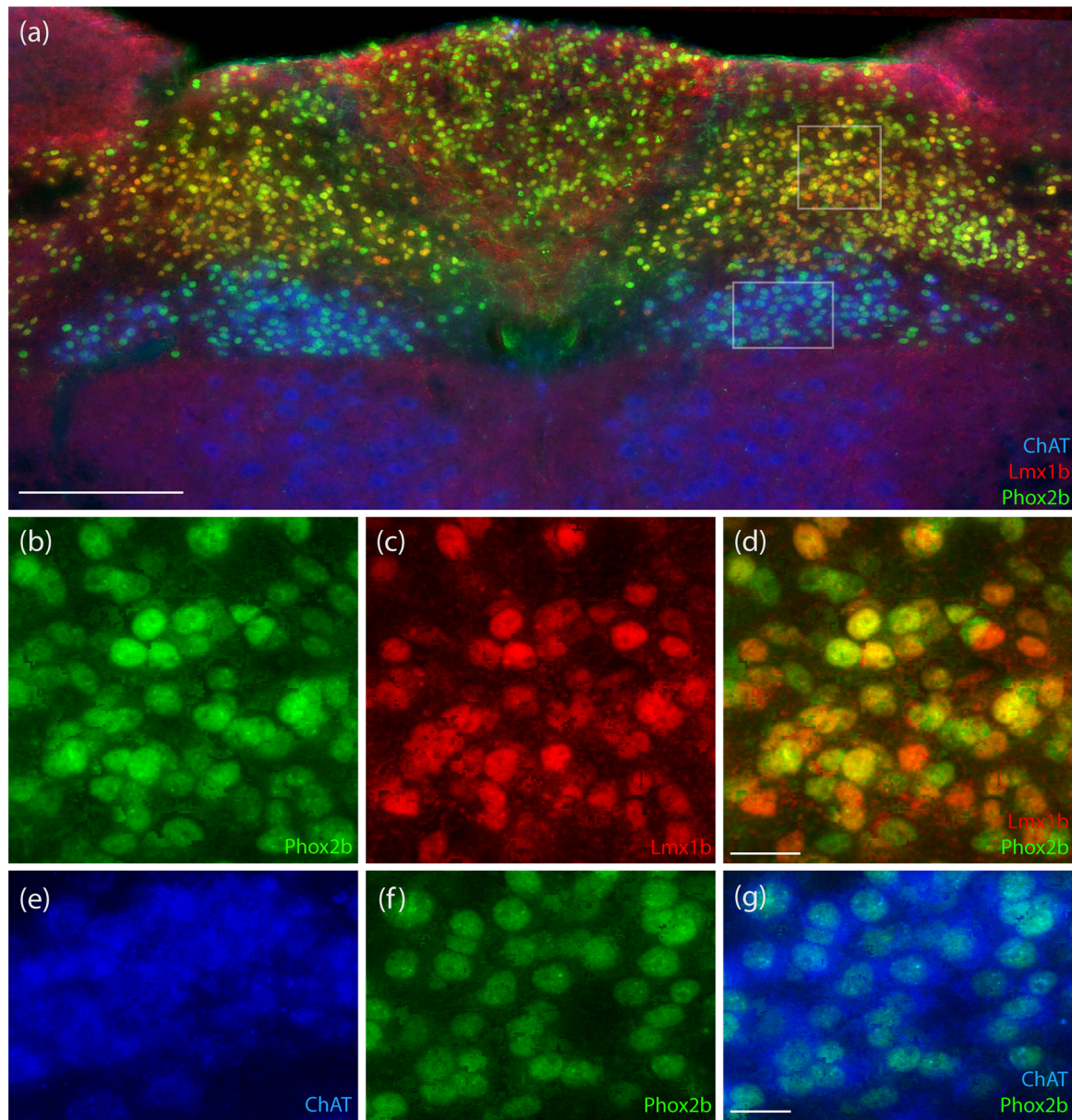
FIGURE 2 | Immunofluorescence labeling for Phox2b (green), Lmx1b (red), and ChAT (blue) in the dorsomedial medulla (a). The expanded inset from the NTS (b–d) highlights the extensive co-expression of Lmx1b and Phox2b. The expanded inset from the DMV (e–g) highlights the uniform co-expression of Phox2b in cholinergic DMV neurons, which have cytoplasmic immunoreactivity for choline acetyltransferase (ChAT). In this region, as reported previously (Gasparini et al. 2019; Kang et al. 2007), Phox2b and ChAT co-localized exclusively in the DMV, and ChAT-immunoreactive (blue) neurons in the hypoglossal nucleus lacked both transcription factors. Scale bar in (a) is 200 μm. Scale bars in (d) and (g) are 20 μm and apply to panels in the same rows.

Consistent with our findings, and with previously published information (Gasparini et al. 2019; Geerling, Chimenti, and Loewy 2008; Kang et al. 2007; Stornetta et al. 2006), the ABCA brain-wide UMAP includes a large subset of neurons expressing *Phox2b* (Figure 9a–c). Within this *Phox2b* macropopulation, small subsets express cholinergic marker genes, including *Chat* (blue arrow in Figure 9d), identifying them as members of the DMV, nucleus ambiguus, and hindbrain motor nuclei (Gasparini et al. 2019; Kang et al. 2007; Pattyn, Hirsch, et al. 2000). Most other neurons in the *Phox2b* macropopulation co-express the vesicular glutamate transporter *Slc17a6*/Vglut2 (Figure 9e), and in the ABCA taxonomy, these neurons form a large subset of a class designated "24 MY Glut" (medullary glutamatergic neurons).

Within this *Slc17a6+Phox2b* macropopulation, one tiny island of cells expresses the vesicular GABA transporter (*Slc32a1*/Vgat; red arrow in Figure 9f) with little to no co-expression of the GABA synthetic enzymes *Gad1* and *Gad2* (not shown).

Also consistent with previously published results (Dai et al. 2008; Gasparini et al. 2019; Gray 2013; Guo et al. 2008; Karthik et al. 2022; Z. R. Liu et al. 2010; Miller et al. 2012; Zhao et al. 2006), the ABCA brain-wide UMAP includes a large subset of neurons expressing *Lmx1b* (Figure 9g). In contrast to *Phox2b*, *Lmx1b* is expressed in not only "24 MY Glut" but also the ABCA classes designated "14 HY Glut" (hypothalamic glutamatergic neurons in subclasses 134, 135, and 136, which include previously identified
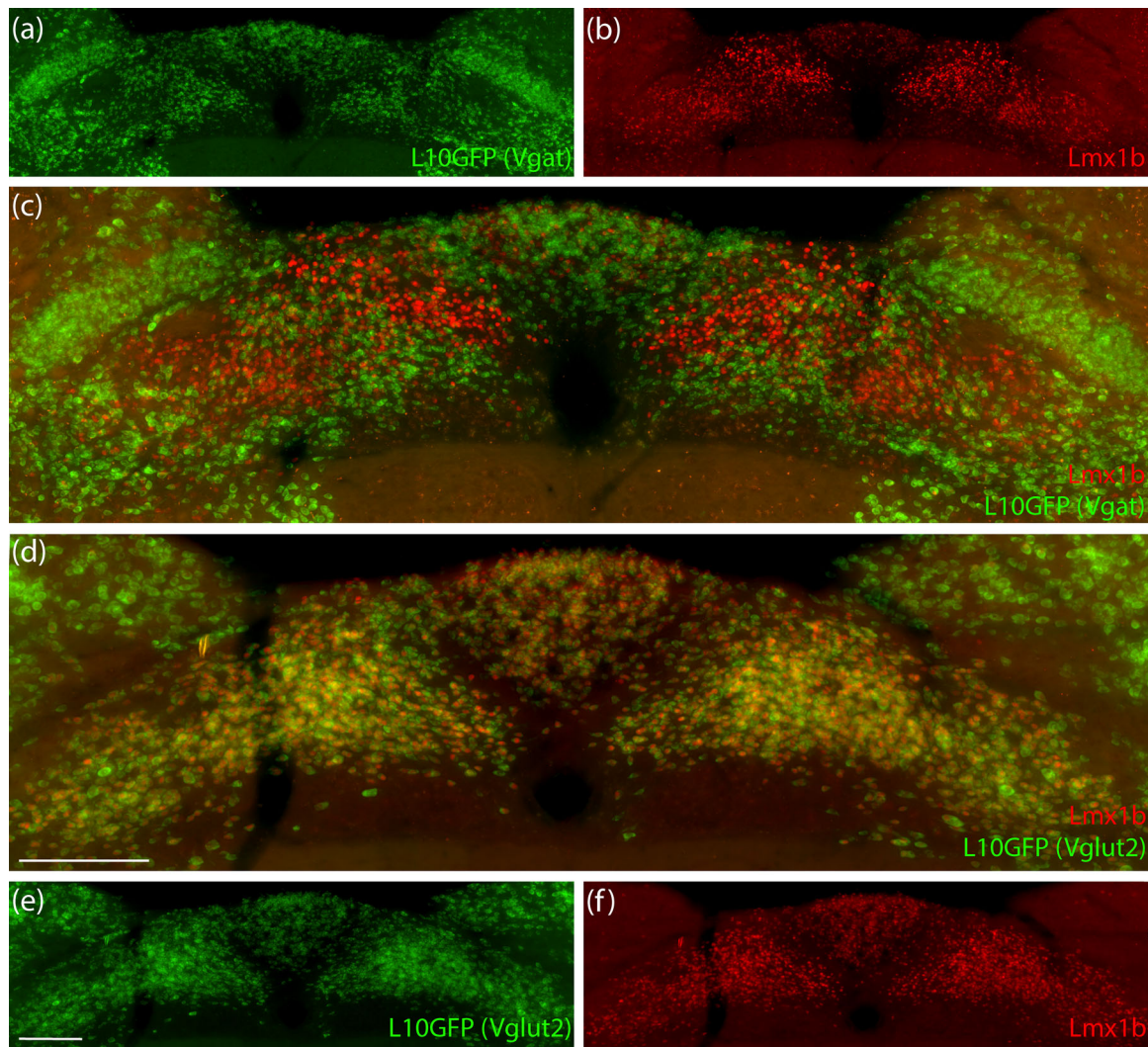
FIGURE 3 | Immunofluorescence labeling for the transcription factor Lmx1b (red) in mice expressing an L10GFP Cre-reporter (green) for *Slc32a1*/Vgat (a-c) or *Slc17a6*/Vglut2 (d-f). Scale bars in (d) and (e) are 200 μm and apply to remaining panels of similar size.

neurons in the subthalamic and parasubthalamic nuclei; Dai et al. 2008), "21 MB Dopa" (midbrain dopaminergic neurons; Dai et al. 2008; Guo et al. 2008), "22 MB-HB Sero" (midbrain and hindbrain serotonergic neurons; Dai et al. 2008; Zhao et al. 2006), and "23 P Glut" (pontine glutamatergic neurons, including a large subset of neurons in the parabrachial nucleus; Karthik et al. 2022). All *Lmx1b* neurons outside the dopaminergic and serotoninergic subsets are glutamatergic (all express *Slc17a6*/Vglut2, and none express the vesicular GABA transporter *Slc32a1*/Vgat).

A distinct subset of these *Lmx1b* glutamatergic neurons co-expresses *Phox2b*. This intersectional subset (*Lmx1b+Phox2b*) includes most of the *Phox2b* macropopulation (Figure 9h), but none of the cholinergic *Phox2b* neurons. This *Lmx1b* co-expressing subset also excludes several glutamatergic subsets of *Phox2b*-expressing neurons (ABCA clusters 4475–4483 and 4485–4489), which presumably include the *Lbx1*/*Phox2b* co-expressing neurons distributed along the ventral hindbrain surface (Cui et al. 2024; Hernandez-Miranda et al. 2018). All the neurons we identified histologically (above) are readily identifiable in the ABCA dataset as mutually exclusive subpopulations of the *Lmx1b+Phox2b* intersectional macropopulation. Specifically, we

found a solitary "peninsula" of neurons expressing *Hsd11b2*, which encodes HSD2 (green arrow in Figure 9i). We also found a separate swath of neurons expressing *Pou3f1* (arrow in Figure 9j), and multiple clusters of neurons expressing the norepinephrine transporter *Slc6a2* (Figure 9k), all of which are mutually exclusive with *Hsd11b2* and *Pou3f1*.

3.6 | Additional Subpopulations in the Subpostremal, Dorsal, and Lateral NTS

Having confirmed that these ABCA transcriptomic data align with our histologic results, we explored this dataset for additional neurotransmitter markers, neuropeptides, transcription factors, and other genes expressed within the *Lmx1b+Phox2b* intersectional macropopulation. We began by examining genes and proteins familiar from our previous work (Gasparini et al. 2019; Geerling, Kawata, and Loewy 2006) and neuroanatomical literature involving the NTS (Armstrong et al. 1981; C. Chen et al. 1999; Herbert and Saper 1990; Kivipelto 1991; Riche et al. 1990; Yamazoe et al. 1984; Zheng et al. 2015). We also examined genes annotated in the ABCA taxonomy as
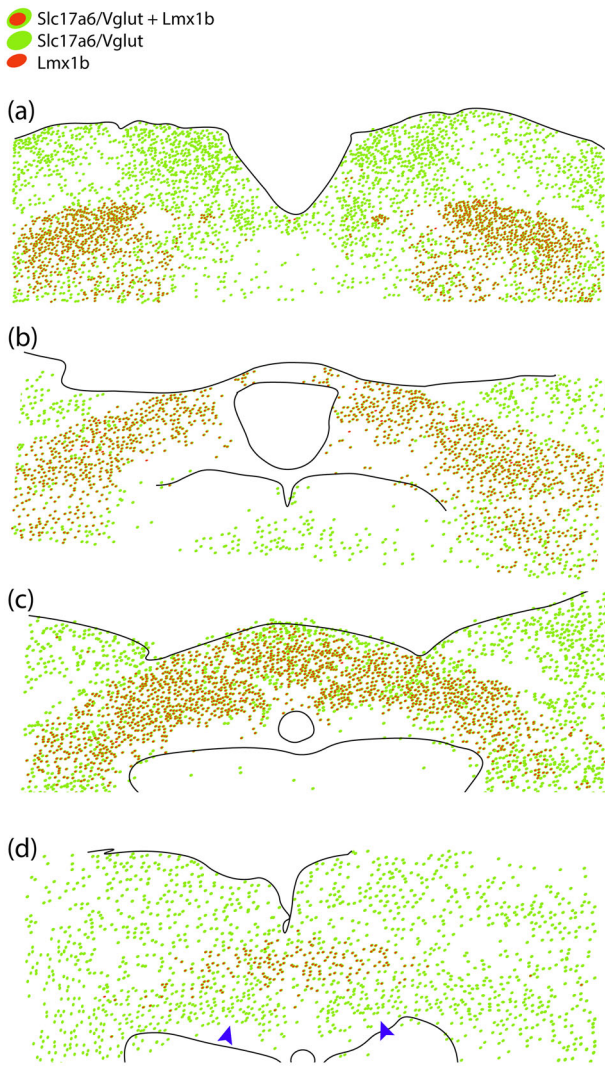
Slc17a6/Vglut + Lmx1b
Slc17a6/Vglut
Lmx1b

FIGURE 4 | Rostral-to-caudal (a–d) plots of L10GFP Cre-reporter expression (for *Slc17a6*/Vglut2) and nuclear immunolabeling for Lmx1b in the dorsomedial medulla. Blue arrowheads in panel (d) highlight a band of putatively glutamatergic neurons that lack Lmx1b in the ventral, far-caudal NTS. Scale bar is 100 μm and it applies to all panels.

potential markers for clusters of glutamatergic neurons in the hindbrain.

Overall, neurons in the intersectional *Lmx1b+Phox2b* macropopulation do not express serotonin or dopamine reuptake transporter genes (*Slc6a2*, *Slc6a4*). However, overlapping subsets of this macropopulation do express catecholaminergic markers, including dopa decarboxylase (*Ddc*), dopamine beta-hydroxylase (*Dbh*), and the vesicular monoamine transporter (*Slc18a2*), in addition to the norepinephrine transporter (*Slc6a2*, above). All subsets expressing these catecholaminergic marker genes co-express the vesicular glutamate transporter (*Slc17a6*/Vglut2) and lack the vesicular GABA transporter (*Slc32a1*/Vgat).

Several other genes, including *Adcyap*, *Cartpt*, *Cck*, *Gad2*, *Gal*, *Nmu*, *Nts*, *Penk*, *Phox2a*, *Slc17a8*, *Sst*, and *Tac1*, had complex and often overlapping patterns of expression that we will not describe in detail here. However, a small number of neuropeptide genes

appear to distinguish mutually exclusive subsets of NTS neurons. For example, strong expression of *Npff* (neuropeptide FF) identifies a distinct island of neurons (Figure 9m), and this *Npff* island includes an upper peninsula with strong co-expression of *Grp* (Figure 9n).

We localized *Npff* mRNA to a subpopulation of neurons in the subpostremal NTS, whose distribution extends into the dorsomedial NTS, just lateral to the rostral edge of the area postrema, where small subset co-expressed *Grp* (Figure 10a–c). This distribution of *Npff*-expressing neurons resembled previous descriptions of NPFF immunoreactivity in rats (Kivipelto 1991) and Cre-reporter expression in mice (Quillet et al. 2023). Also, the subpostremal component of this subpopulation resembled the distribution of a Cre-reporter for *Sctr* (secretin receptor) reported in mice (figure 3G of Y. Liu et al. 2023), and we observed in the ABCA dataset that *Sctr* identified the remaining (non-*Grp*) part of the *Npff* island (Figure 9o). Therefore, we labeled *Sctr* in combination with *Npff*, followed by HSD2 immunolabeling, which confirmed that both populations are mutually exclusive with and dorsal to the HSD2 neuron distribution (Figure 11). *Sctr*-expressing neurons formed a "V" shape in the subpostremal NTS, and virtually all of these neurons co-expressed *Npff* (Figure 11). NTS neurons co-expressing *Npff* and *Sctr* extended rostrally, up to the level of the obex, and we found additional, strong expression of *Sctr* in a subset of DMV neurons and in the ependymal cells lining the fourth ventricle and central canal of the spinal cord (Figure 12).

At the same level, labeling *Pdyn* mRNA revealed an additional subpopulation of neurons that were mutually exclusive with *Npff* and *Sctr* and had a more lateral distribution (Figure 12). Caudal to this level, we found fewer and more diffuse neurons, including a small number of *Pdyn*-expressing neurons in the DMV (identified previously in Tao et al. 2021), and a small number of ependymal cells expressing *Pdyn* in the midline of the fourth ventricle. However, at this relatively rostral level, the prominent cluster of *Pdyn*-expressing neurons occupied a more lateral subregion, near the solitary tract, which included subregions previously described in rats as "interstitial," "intermediate," "dorsolateral," and "ventrolateral" subnuclei (Herbert, Moga, and Saper 1990; Kalia and Sullivan 1982).

3.7 | Caudal NTS

A well-known population of neurons in the caudal hindbrain produces glucagon-like peptide 1 (GLP-1), which is encoded by the gene *Gcg*. *Gcg*-expressing neurons distribute through the caudal reticular formation and into the lateral edge of the caudal NTS, and they reduce food intake (Holt, Richards, et al. 2019; Kreisler and Rinaman 2016; Ly et al. 2023). They are often referred to as NTS neurons, so we were surprised to find in the ABCA that *Gcg* expression identifies an island of neurons that lack both *Lmx1b* and *Phox2b* (Figure 9p). Intrigued by this finding, and having identified a ventral, far-caudal population of glutamatergic neurons lacking these transcription factors (Figures 4 and 5), we labeled *Gcg* in combination with *Phox2b*. At levels caudal to the area postrema, extending ventrolaterally into the caudal medullary reticular formation, *Gcg* expression distinguished a small subset of medium-large neurons along the ventrolateral
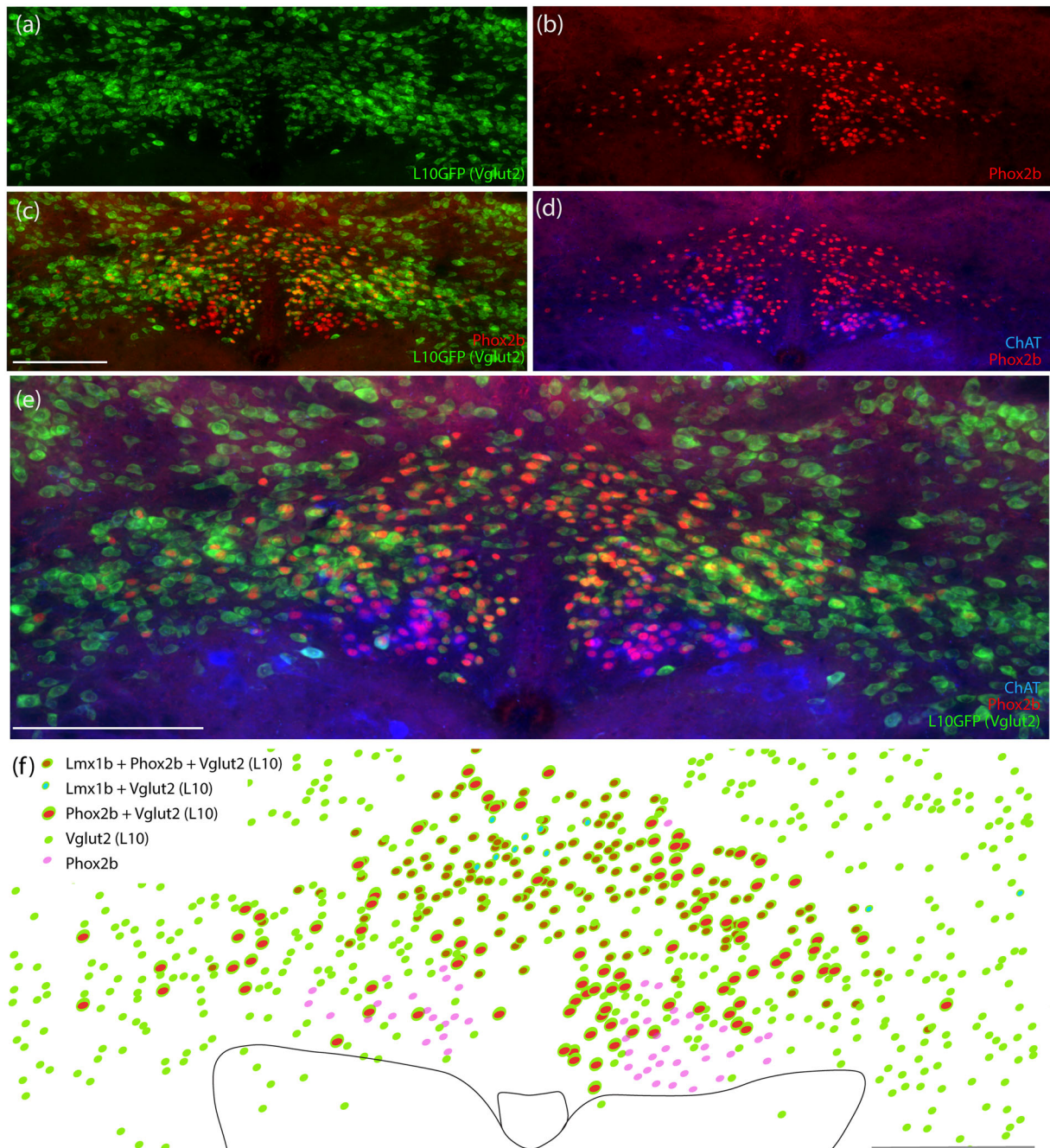
FIGURE 5 | Phox2b (red) and ChAT (blue) immunofluorescence in mice expressing the L10GFP Cre-reporter for *Slc17a6*/Vglut2 (green), at a level caudal to the area postrema. This marker combination confirmed that *Phox2b*-expressing neurons form separate glutamatergic and cholinergic subsets in the NTS and DMV (a–e) and revealed that many glutamatergic neurons lack Phox2b in the caudal-ventral NTS and adjoining reticular formation. (f) Plotting Lmx1b- and Phox2b-immunoreactive neurons at this caudal level, along with the L10GFP Cre-reporter for *Slc17a6*/Vglut2, revealed a dorsal subset of glutamatergic neurons expressing both transcription factors (green with brown), along with a glutamatergic subset expressing only Phox2b (green with red), a moderate number of glutamatergic neurons lacking both transcription factors (green), and a smaller, dorsal subset with only Lmx1b (green with cyan), along with nonglutamatergic Phox2b-expressing neurons in the DMV (pink dots). Scale bars are 200 μm and apply to remaining panels of similar size.

fringe of the NTS. In both the NTS and the reticular formation, *Gcg*-expressing neurons intermingled with neurons expressing *Phox2b*, but we did not find any neurons co-expressing *Gcg* and *Phox2b* (Figure 13a–d). *Gcg*-expressing neurons co-express *Slc17a6*/Vglut2 in the ABCA dataset (consistent with previous findings in the rat hindbrain; Zheng et al. 2015), and we found uniform co-localization between a Cre-reporter for *Slc17a6*/Vglut2

and *Gcg* mRNA (Figure 13e–g). Nearby in the caudal NTS, a subset of noradrenergic (*Slc6a2*-expressing) neurons co-express the neuropeptide *Prlh* (prolactin-releasing hormone; C. Chen et al. 1999; Holt and Rinaman 2022; Ly et al. 2023) and the calcitonin receptor *Calcr* (W. Cheng et al. 2021). Unlike *Gcg*, *Prlh*-expressing neurons do co-express *Phox2b* (Figure 9l), but their *Lmx1b* expression is low and variable in the ABCA dataset. Thus,
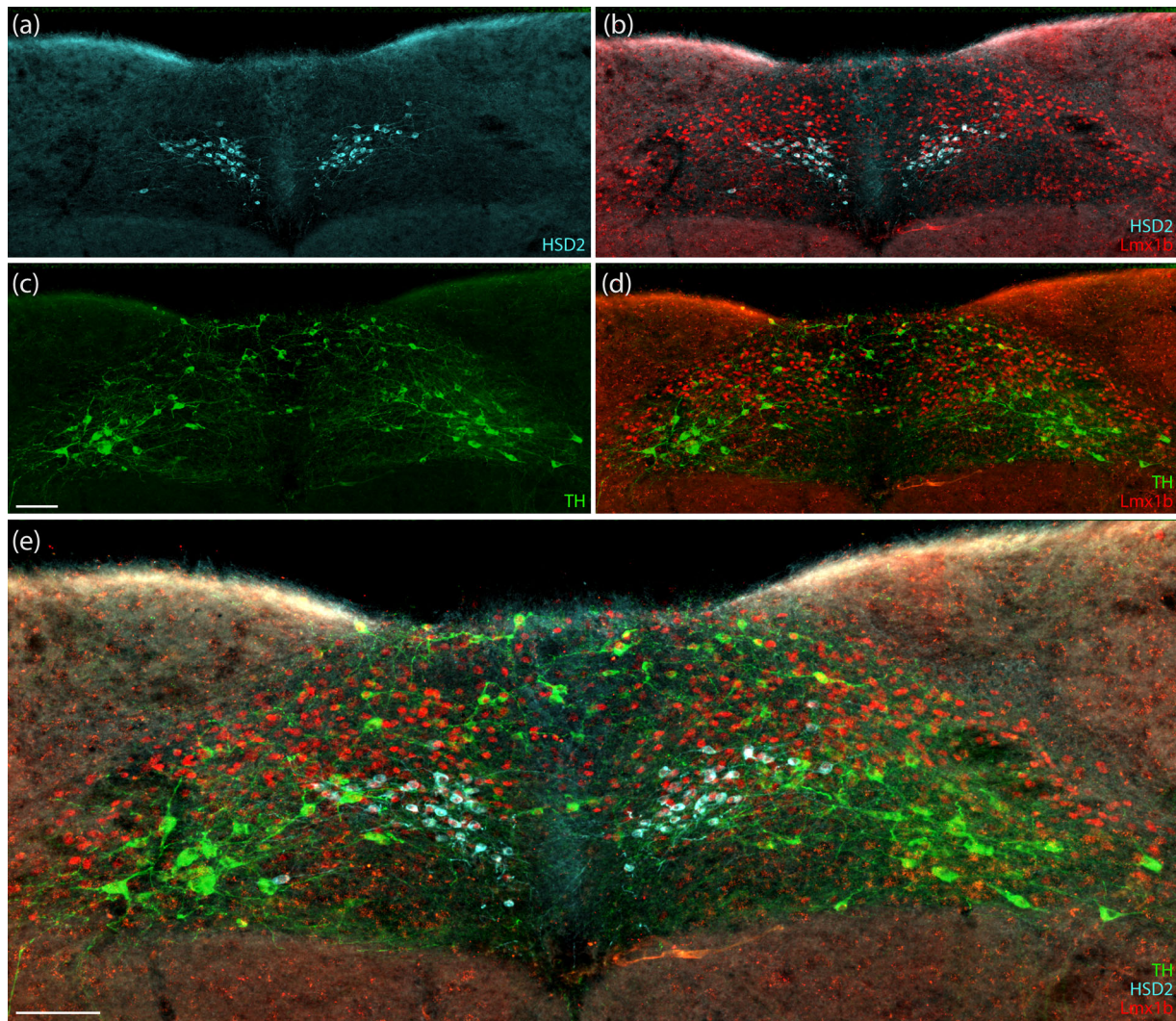
FIGURE 6 | (a–e) Immunofluorescence labeling for the enzymes 11-beta-hydroxysteroid dehydrogenase type 2 (HSD2, ice-blue) and tyrosine hydroxylase (TH, green), in combination with Lmx1b nuclear immunolabeling (red). Scale bars in (c) and (e) are 100 μm, and scale bar in (c) applies to remaining panels.

the caudal-ventral band of glutamatergic neurons identified here as lacking either *Lmx1b* or both *Lmx1b* and *Phoxb2* (Figures 4 and 5) include a *Prlh*-expressing subset that lacks *Lmx1b* and a *Gcg*-expressing subset that lacks both *Lmx1b* and *Phox2b*.

4 | Discussion

Our results establish the groundwork for a molecular ontology of NTS neurons. We present a curated overview of molecular markers that identify and distinguish neurons in this region, including novel and previously identified subpopulations (Figure 14). Information presented here has immediate practical implications and opens opportunities for neuroscience research aimed at linking specific NTS neurons to specific interoceptive functions.

4.1 | Molecular Markers Identify NTS Neurons and Distinguish Subpopulations

Hindbrain neurons develop along rostrocaudal segments known as rhombomeres. Cells in each segment express combinations

of transcription factors that, along with positional cues provided by secreted factors along the dorsoventral axis, determine the specification, migration, differentiation, and circuit connections of all hindbrain neurons (Hernandez-Miranda, Müller, and Birchmeier 2017; Hirsch et al. 2021). We know very little about which transcription factor combinations are responsible for the development of specific NTS subpopulations, but pivotal findings in this region include observations that the NTS fails to develop in mice with deletion of either *Phox2b* or *RnxTlx3* (Dauger et al. 2003; Qian et al. 2001). *Phox2b* is also necessary for the development of noradrenergic neurons, peripheral autonomic ganglia, parasympathetic premotor neurons, and a subset of motor neurons and glutamatergic interneurons in the hindbrain (Pattyn, Goridis, and Brunet 2000; Pattyn, Hirsch, et al. 2000; Pattyn et al. 1999).

Beyond this, we know little about factors specifying connections and functions of NTS neurons. Learning that *Lmx1b* expression together with *Phox2b* selectively identifies glutamatergic NTS neurons extends previous neuroanatomical studies that highlighted either *Phox2b* (Kang et al. 2007) or *Lmx1b*
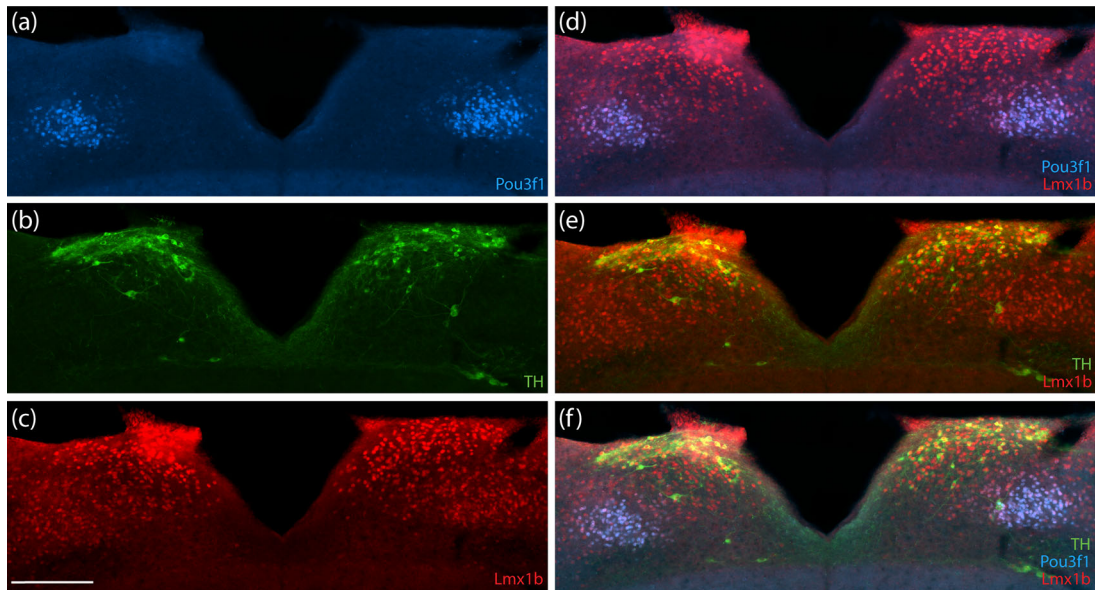
FIGURE 7 | (a–f) Immunofluorescence labeling for the transcription factors Pou3f1 (blue) and Lmx1b (red), along with TH (green) in the intermediate NTS, rostral to the obex. Scale bar is 200 μm and applies to all panels.
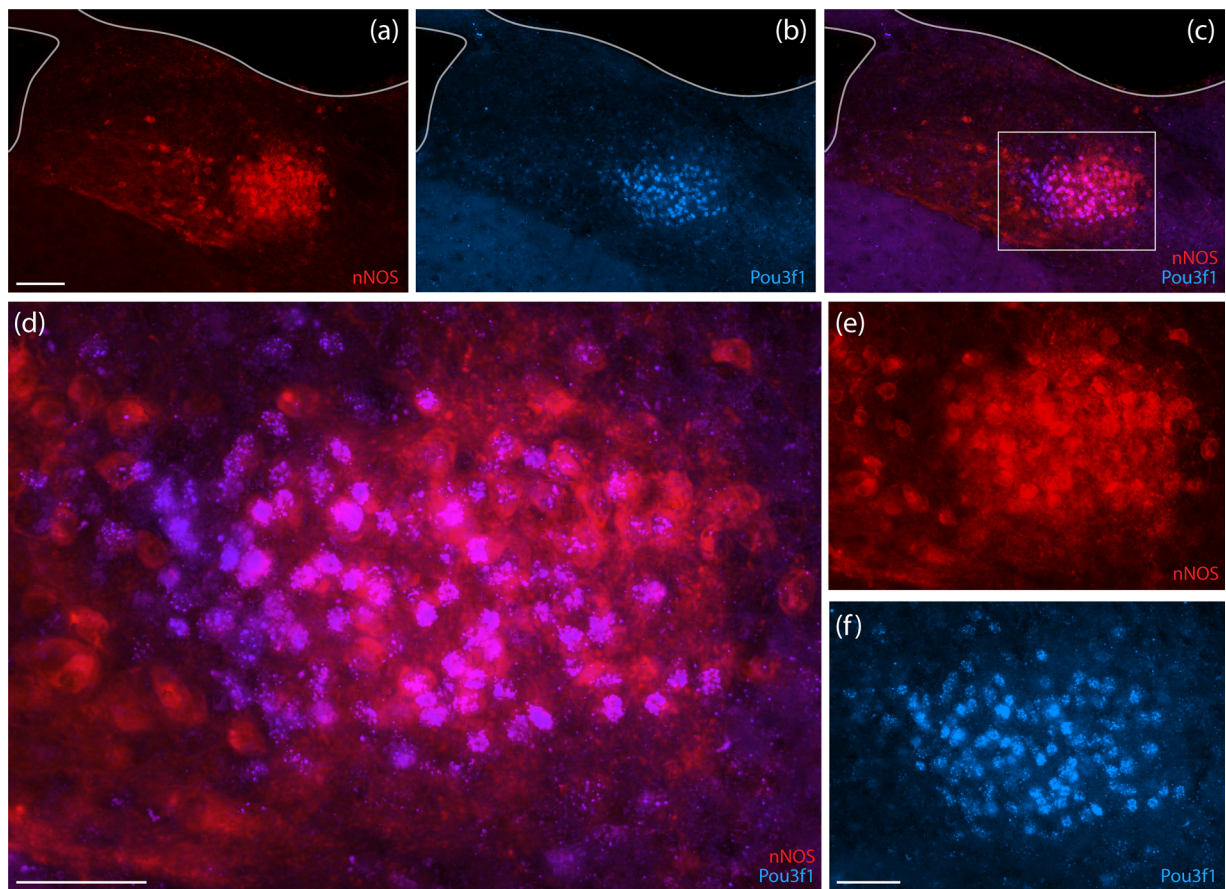

FIGURE 8 | (a–f) Immunofluorescence labeling for Pou3f1 (blue, nuclear immunoreactivity) and neuronal nitric oxide synthase (nNOS, red, cytoplasmic immunoreactivity). Scale bar in (d) is 50 μm. Scale bars in (a) and (f) are 100 and 50 μm, respectively, and apply to remaining panels of similar size.
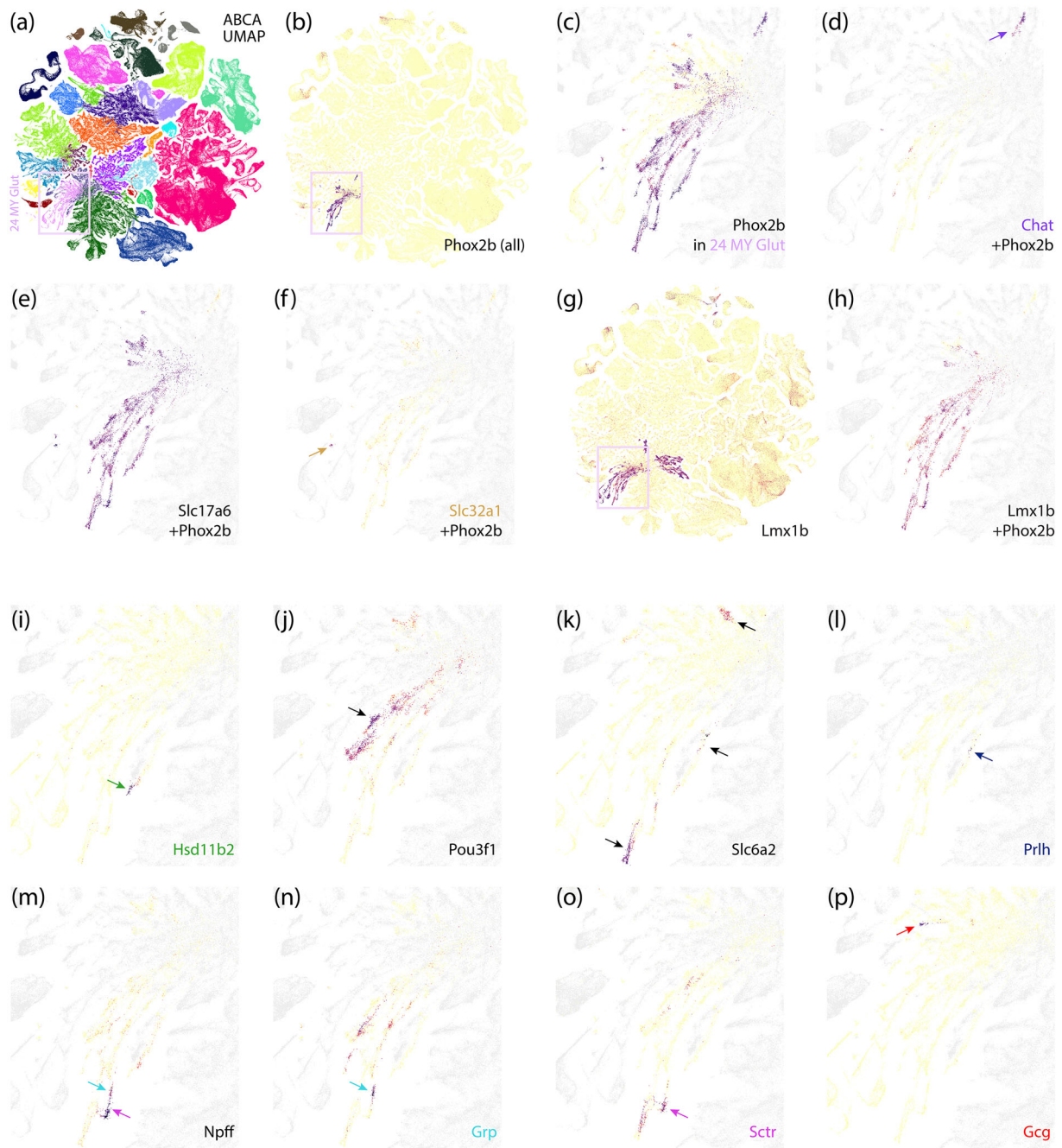
FIGURE 9 | Single-cell transcriptomic analysis from the Allen Brain Cell Atlas (ABCA). (a) Uniform manifold approximation and projection (UMAP) of the approximately four million combined neurons in this public dataset, with medullary glutamatergic neurons (ABCA class "24 MY Glut") highlighted in pale lilac. (b–p) See Results text for details.

(Dai et al. 2008) in this region. Complementing the necessity of *Phox2b* for noradrenergic neuron development, *Lmx1b* plays a critical role in the specification and maintenance of serotoninergic and dopaminergic neurons (Ding et al. 2003; Guo et al. 2008; Smidt et al. 2000; Zhao et al. 2006). *Lmx1b* is also important for maintaining the glutamatergic identity of neurons in the dorsal horn of the spinal cord and principal trigeminal sensory nucleus (Szabo et al. 2015; Xiang et al. 2012). A transcription factor that is co-expressed with *Lmx1b*, *Tlx3* (Dai et al. 2008), is also necessary for specifying glutamatergic over GABAergic identity in the dorsal horn of the spinal cord (L. Cheng et al. 2004, 2005).

Tlx3 is also required for the development of *Phox2b*-expressing neurons in the NTS but not in the DMV (Qian et al. 2001). ABCA data confirm broad co-expression of *Tlx3* with *Lmx1b*, and we hypothesize that these two transcription factors specify and maintain the glutamatergic identity of *Phox2b*-expressing neurons in the NTS.

In contrast, *Phox2b*-expressing neurons in the nucleus ambiguus and DMV lack *Lmx1b* and maintain a cholinergic identity. We also identified a small population of *Phox2b*-expressing glutamatergic neurons that lack *Lmx1b*. These neurons, in the caudal NTS, are
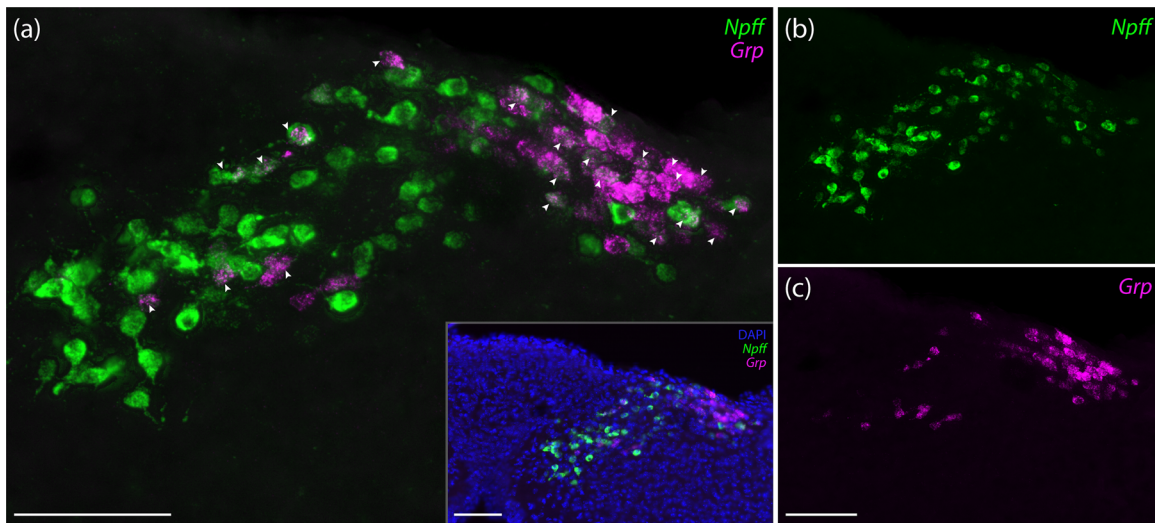
FIGURE 10 | (a–c) *Npff* (green) and *Grp* (magenta) mRNA labeling in subpostremal and dorsomedial parts of the NTS. Arrowheads highlight the subset of neurons co-expressing *Npff* and *Grp*. All scale bars are 100 μm, and the scale bar in (c) also applies to (b).
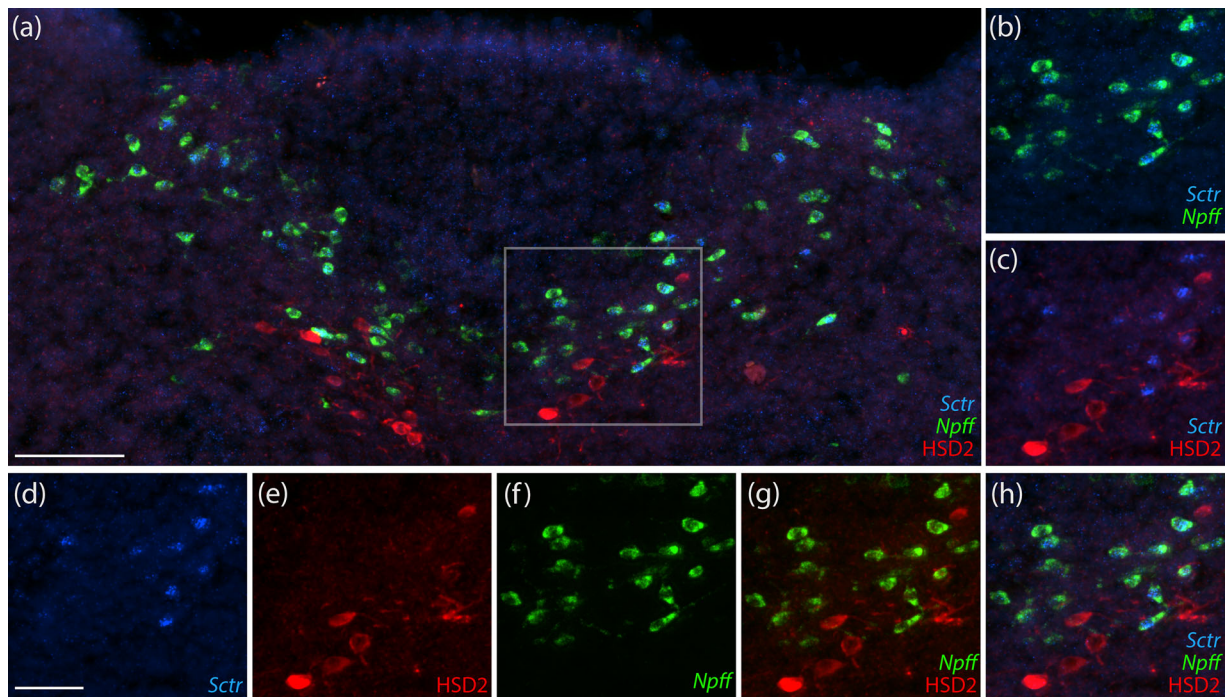

FIGURE 11 | *Npff* (green) and *Sctr* (blue) mRNA labeling followed by HSD2 immunofluorescence labeling in the medial NTS, ventral to the area postrema. Many neurons co-express *Sctr* and *Npff* (b), but neither are co-expressed with HSD2 (c, g, h). Scale bar in (a) is 100 μm. Scale bar in (d) is 50 μm and applies to all remaining panels (b–h).

sandwiched between the larger *Lmx1b+Phox2b* macropopulation dorsally and the cholinergic DMV *Chat+Phox2b* population ventrally. They include a *Prlh*-expressing subset of A2 noradrenergic neurons (C. Chen et al. 1999), which play a role in feedback-inhibition of appetite (W. Cheng et al. 2021; Holt and Rinaman 2022; Ly et al. 2023). We do not know the developmental lineage of these neurons or the functional implications of lacking *Lmx1b*, nor do we know the lineage of neighboring neurons that lack both *Lmx1b* and *Phox2b*—including the *Gcg*-expressing (GLP-1) neurons, which play a related role in appetite feedback (Gaykema

et al. 2017; Holt, Richards, et al. 2019; Holt and Rinaman 2022; Kreisler and Rinaman 2016; Vrang et al. 2003). Nonetheless, this information has practical value. For example, planning experiments in *Lmx1b*-Cre mice (or any other *Lmx1b*-driven recombinase strain) to access NTS neurons would exclude these caudal-ventral subsets. Likewise, experiments using *Phox2b*-Cre mice would exclude *Gcg*/GLP-1 neurons and surrounding glutamatergic neurons that lack *Phox2b* in this caudal region. Overlapping subpopulations of neurons linked to appetite control express the calcitonin receptor *Calcr* or leptin receptor *Lepr* (W.
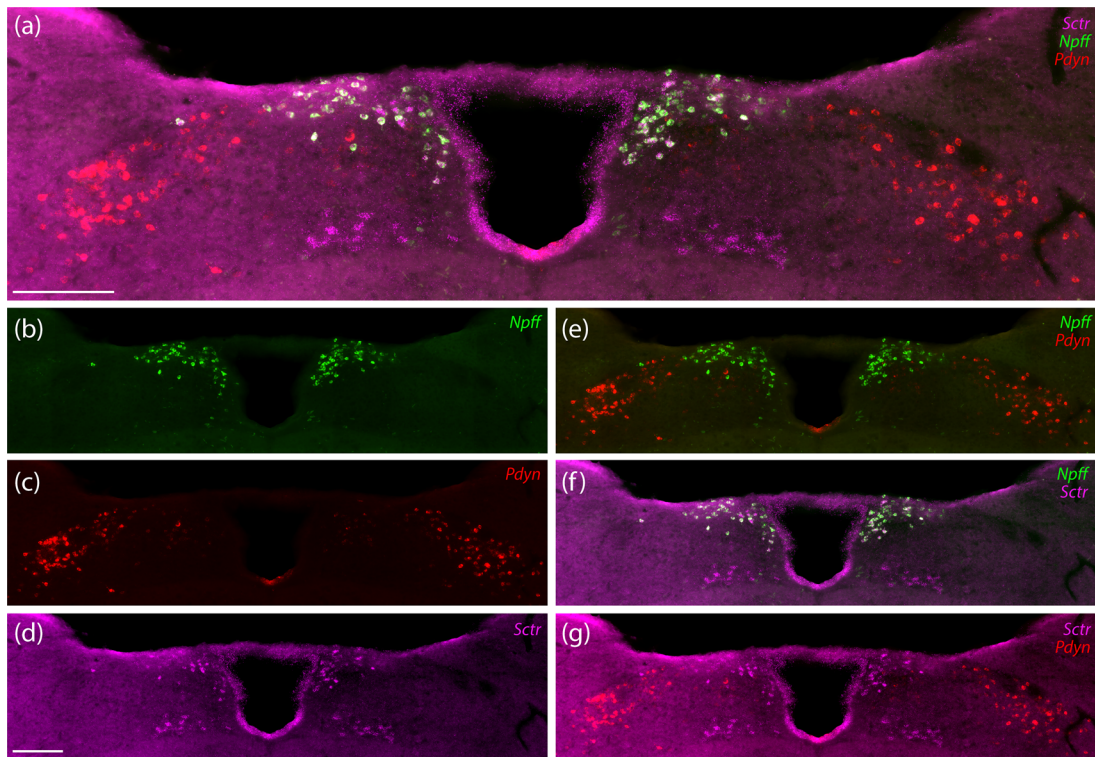
FIGURE 12 | (a–g) *Npff* (green) combined with *Sctr* (magenta) and *Pdyn* (red) mRNA labeling at the level of the obex. Many neurons co-express *Npff* and *Sctr*. Additional *Sctr* expression was evident in the ependymal cells lining the fourth ventricle and in a small number of DMV neurons. At this level, most *Pdyn* neurons clustered near the solitary tract in the dorsolateral NTS, separate from neurons co-expressing *Npff* and *Sctr*. Scale bar in (a) is 200 μm. Scale bar in (d) is 200 μm and applies to remaining panels (b–g).

Cheng, Gonzalez, et al. 2020; Qiu et al. 2023), and it is tempting to speculate that a distinct developmental trajectory, revealed by the lack of *Lmx1b* (or lack of both *Lmx1b* and *Phox2b*), specifies patterns of adult gene expression and connectivity that allow a neuron to regulate appetite, rather than one of the autonomic reflex functions classically associated with the caudal NTS. We hypothesize that smaller neurons in the *Lmx1b+* macropopulation control autonomic reflexes via local connections in the hindbrain, while larger, non-*Lmx1b*/non-*Phox2b* neurons at the caudal-ventral fringe of this region control appetite via long-range projections to the upper brainstem and forebrain. The molecular ontology detailed here lays a foundation for raising and testing this and similar questions about connectivity and functions of NTS neurons.

In preliminary studies, we have examined adult expression of a variety of other transcription factors, including those highlighted in previous studies of hindbrain development (Gray 2013; Hernandez-Miranda, Müller, and Birchmeier 2017), without finding any expression patterns as broadly selective for NTS neurons as the intersection of *Phox2b* with *Lmx1b/Tlx3*, and without yet identifying more specific markers for individual NTS subpopulations. Additional subpopulations that are demarcated by more complex combinations of genetic markers may be identified using spatial transcriptomic analysis (K. H. Chen et al. 2015). Given the vital and clinically important functions of neurons in this intricate and diverse region, we hope that the curated molecular ontology provided here will help accelerate work in the NTS, while also highlighting facets where our understanding remains incomplete.

4.2 | Implications for Studying Functionally Distinct NTS Subpopulations

The present results have additional practical implications for studying the connectivity and functions of NTS neurons. As noted above, knowing which genes are co-expressed (and which are not) should guide the selection of recombinase-conditional experimental approaches for targeting specific neurons of interest. For example, the total absence of *Phox2b* mRNA in *Gcg*-expressing (GLP-1) neurons raises the possibility that previous experimental approaches using transgenic *Phox2b*-Cre mice to activate or alter gene expression in this population (Scott et al. 2011; Wang et al. 2015) may not have involved GLP-1 neurons. Both transcriptomic evidence in the ABCA and our in situ evidence confirmed the mutual exclusivity of *Phox2b* and *Gcg*, and these findings complement a previous report that only NTS neurons lacking *Gcg*/GLP-1 expression could be transduced by a virally injected GFP vector with the *Phox2a/Phox2b*-driven promotor PRSx8 (Holt, Richards, et al. 2019). The developmental lineage of *Gcg*/GLP-1 and neighboring glutamatergic neurons that lack *Phox2b* is unknown, so the same consideration may apply to several subtypes of neurons in this ventral-caudal region. Whether or not *Phox2b*-negative populations should be considered part of the NTS is open to debate, but learning more about their (likely distinct) developmental lineage could uncover experimentally and clinically useful information.

More importantly, our results provide a useful framework for the debate over whether and to what extent molecular identity defines functionally discrete subpopulations of neurons in the
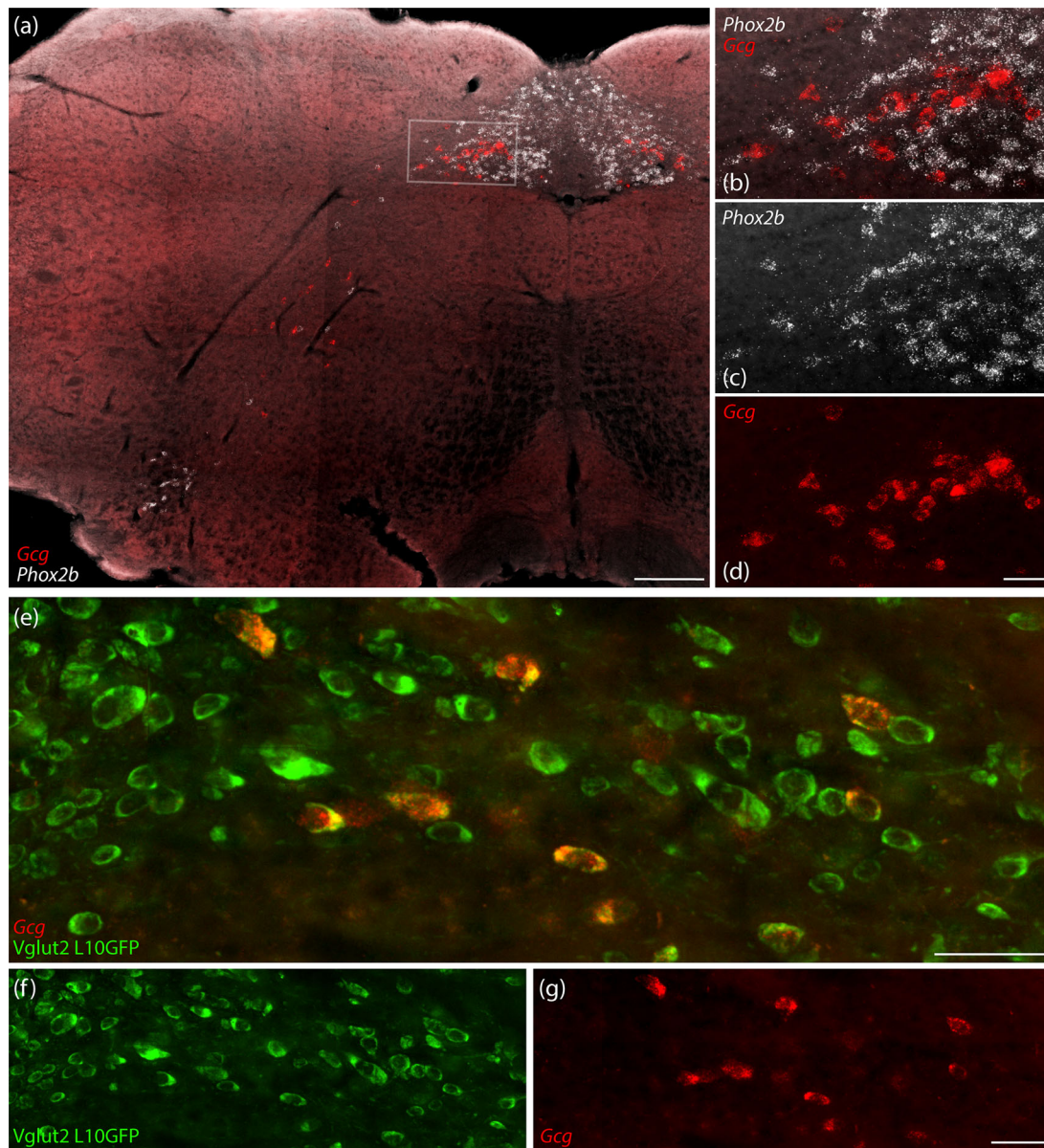
FIGURE 13 | (a–d) *Gcg* (red) and *Phox2b* (white) mRNA labeling in the caudal medulla. No neurons in the NTS or reticular formation co-express *Gcg* and *Phox2b*. (e–g) *Gcg* mRNA expression localizes to relatively large neurons expressing the L10GFP Cre-reporter for *Slc17a6*/Vglut2. Scale bar in (a) is 250 μm. Scale bar in (d) is 50 μm and applies to (b–c). Scale bar in (e) is 50 μm. Scale bar in (g) is 50 μm and applies to (f).

NTS. As detailed above, we can demarcate many subpopulations on the basis of single-gene expression in the adult NTS, and in many other brain regions, molecular identity dictates distinct patterns of connectivity and function. However, a recent study questioned the link between genetic identity and connectivity in the NTS. That study showed that the established mosaic of input from different cranial nerves and visceral systems (Altschuler et al. 1989; Bassi et al. 2022; Contreras et al. 1982; Hamilton and Norgren 1984; Kalia and Sullivan 1982) corresponds to a similar topography of NTS neurons responding to stimulation of different locations along the gastrointestinal tract (Ran et al. 2022). In an attempt to study a link between this viscerotopic pattern and genetically defined subtypes of NTS neurons, the authors injected viral vectors that delivered a non–Cre-dependent calcium indicator and Cre-dependent GFP in several knockin-Cre mouse strains (*Calcr-*, *Cartpt-*, *Chrh2-*, *Gcg-*, *Penk-*, *Pdyn-*, *Sst-*, *Tac1-*, and *Th-*

Cre). Many of these Cre-driver genes—particularly *Cartpt*, *Penk*, *Sst*, and *Tac1*—are expressed broadly, in multiple subpopulations scattered across several NTS subregions, and most of the uniquely expressed genes highlighted above were not used. The authors found responses to mechanical distention of both the stomach and duodenum in GFP-expressing neurons of each strain and interpreted this finding as evidence that the position of a neuron within the NTS may hold more useful information about its input connectivity than the molecular identity of that neuron (Ran et al. 2022). Arguing against this perspective are several examples of marker-defined NTS subpopulations with highly specific connections and distinct functions.

First, the aldosterone-sensitive HSD2 neurons project axons from the NTS to highly specific targets in the upper brainstem and forebrain (Gasparini et al. 2019; Geerling and Loewy 2006;
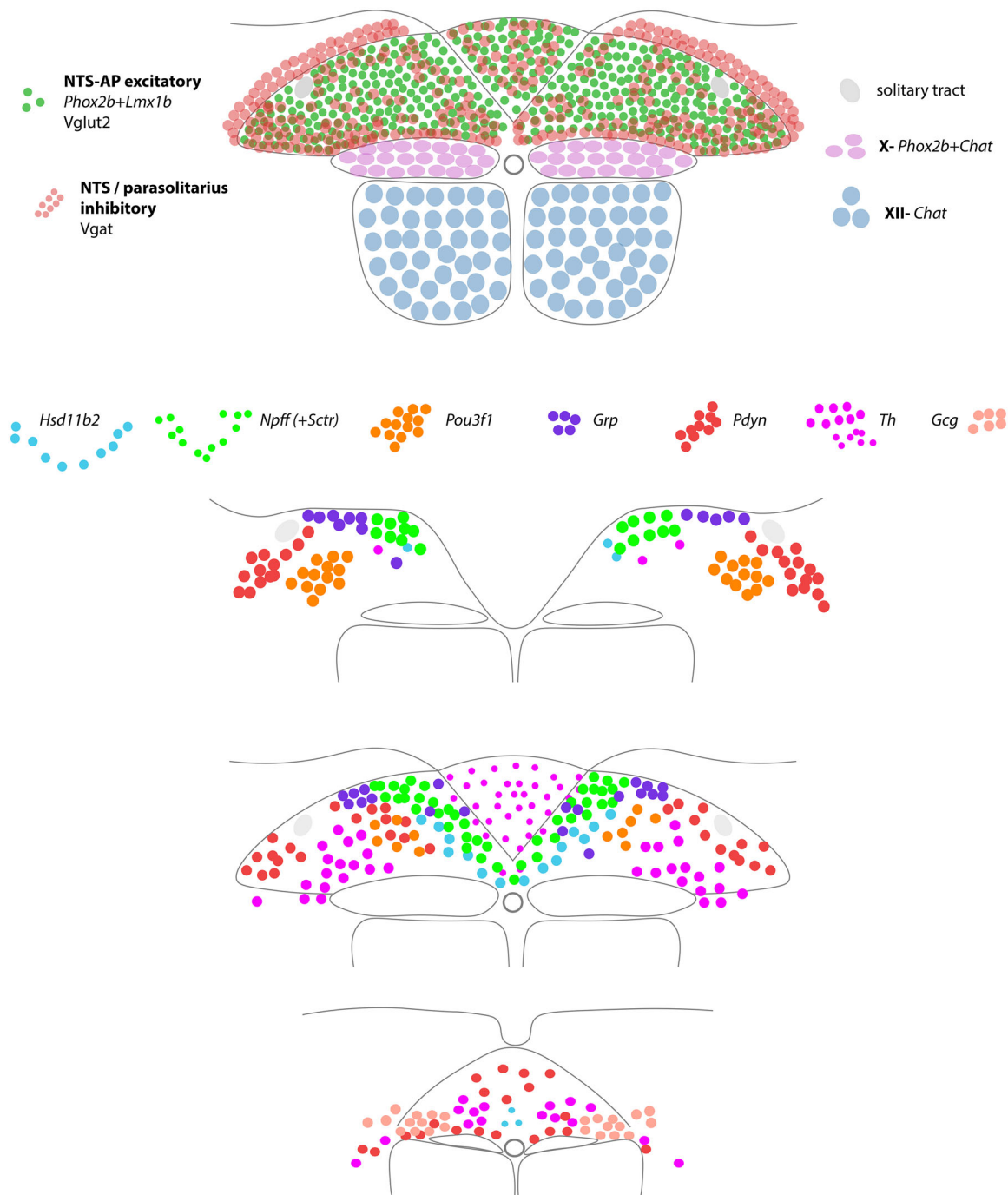
FIGURE 14 | Illustration of molecular markers in the NTS.

Jarvie and Palmiter 2017; Resch et al. 2017). The present results confirm our previous reports in rats and mice showing that this population is distinct from other identified subpopulations of NTS neurons (Gasparini et al. 2019; Geerling, Kawata, and Loewy 2006). Activating *Hsd11b2*-expressing neurons selectively increases sodium appetite (Jarvie and Palmiter 2017; Resch et al. 2017), and removing *Hsd11b2*-expressing neurons from the NTS eliminates aldosterone's ability to increase sodium appetite (Gasparini et al. 2024). Importantly, HSD2 neurons do not receive direct synaptic input from the vagus nerve and do not project axons to regions of the hindbrain that control autonomic reflexes, and activating these neurons has no effect on blood pressure

(Gasparini et al. 2018; Resch et al. 2017). They surround the area postrema, which has an opposing effect on sodium appetite, and molecular-genetic techniques are necessary to study HSD2 neurons, arguing against the utility of topography for determining cell-type/function relationships in this subregion.

Second, separate subpopulations of neurons in the caudal, ventral NTS potently reduce food intake. These neurons express an overlapping variety of molecular markers, including *Calcr*, *Cartpt*, *Cck*, *Gcg*, *Lepr*, and *Prlh*. Stimulating *Cck*-expressing NTS neurons that send output to the lateral parabrachial nucleus has an aversive impact and reduces food intake

(Qiu et al. 2023; Roman, Sloat, and Palmiter 2017), while *Gcg*/*Lepr* and *Calcr*/*Prlh* neurons reduce appetite without an aversive effect, suggesting that their function may be to promote postprandial satiation (W. Cheng, Gonzalez, et al. 2020; W. Cheng, Ndoka, et al. 2020; W. Cheng et al. 2021; Gaykema et al. 2017). Further, *Prlh*- and *Gcg*-expressing populations appear to relay separate oral or gastroduodenal nutrient and stretch-sensory information, and activating them produces either prolonged inhibition of (*Gcg*) or brief pauses in (*Prlh*) food intake (Ly et al. 2023). Stimulating a catecholaminergic *Dbh*/*Npy*-expressing subset of NTS neurons increases food intake (J. Chen et al. 2020), consistent with a separate report that rostral catecholaminergic (*Th*-expressing) NTS neurons increase hunger, while caudal *Th*-expressing neurons (presumably including the *Calcr*/*Prlh* subset) reduce food intake (Aklan et al. 2020; Sayar-Atasoy et al. 2023). Supporting the value of topographical information is the finding that neurons in the area postrema expressing the GLP-1-receptor (*Glp1r*) inhibit appetite with adverse hedonic effects, while those in the underlying NTS lack the averse hedonic affect (Huang et al. 2024).

Third, the distribution of *Pdyn*-expressing neurons we identified above, surrounding the solitary tract at intermediate levels of the lateral NTS subdivision, bears striking resemblance to the terminal distribution in rats of vagal axons arriving from the larynx (figure 12B of Altschuler et al. 1989). This afferent/cell-type correspondence was not investigated in the calcium imaging experiments described above (Ran et al. 2022), and it strongly suggests a role of these lateral, *Pdyn*-expressing neurons in gag, swallow, or cough reflexes. The cough reflex was linked to *Tac1*-expressing neurons in a subsequent study (Gannot et al. 2024), but *Tac1* is expressed in multiple clusters of NTS neurons, and it is unclear which subset promotes cough-like reflex behavior.

Fourth, one of the most clear-cut input–output relationships in the entire brainstem is the close correspondence between vagal axons arriving from the esophagus and esophageal premotor neurons located in the prominent, round "central subnucleus" of the NTS (Cunningham and Sawchenko 1989; Herbert, Moga, and Saper 1990; Wiedner, Bao, and Altschuler 1995). We replicated the previously identified distribution of neurons expressing the nuclear transcription factor *Pou3f1* in this location and showed that a prominent, round subset of these neurons expresses *Nos1*/nNos, which was previously shown to identify esophageal premotor neurons in rats (Wiedner, Bao, and Altschuler 1995). *Pou3f1*-expressing NTS neurons receive input from vagal sensory neurons that express *Prox2*/*Runx3* and innervate the upper gastrointestinal tract (Lowenstein et al. 2023). While awaiting functional confirmation, these neuroanatomical features strongly suggest that these *Pou3f1*/*Nos1* neurons play a highly specific role in reflex control of esophageal motility.

To our knowledge, no subpopulation markers have been identified for gustatory-relay neurons in the rostral NTS. Similarly, no cell-type–specific markers have been identified for NTS neurons controlling several well-known autonomic reflexes, including the baroreflex, chemoreceptor reflex, gastric vago-vagal reflex, gastro-colic reflex, Hering–Breuer reflex, and vasovagal reflex. Our new findings provide several new candidates as a template for identifying and testing new subpopulations in future work. For example, while we do not yet have a subpopulation-specific marker for these neurons, the prominent population of large

GABAergic (*Slc32a1*/Vgat-expressing) neurons in the ventrolateral NTS may be the "pump cells" that receive slowly adapting stretch receptor input from the lungs and mediate the Hering–Breuer reflex (Ezure and Tanaka 2004). Future work may also narrow down a more specific subpopulation responsible for the "sickness behaviors" and "retching-like behavior" that have been attributed to widespread populations of NTS neurons that express the neuropeptide *Adycap1* and the calcium-binding protein *Calb1*, respectively (Huo et al. 2024; Ilanges et al. 2022).

4.3 | Limitations

Our approach emphasized reproducibility by focusing on genes with stable expression in adult mice. However, some genes are differentially expressed, for example, in a fed vs. fasted condition (Dowsett et al. 2021). One well-known example of variable gene expression is the activity-induced gene *Fos*, which can distinguish a variety of different neurons after specific experimental perturbations that selectively activate a neuron of interest. If any subpopulation of NTS neurons activates its unique pattern of gene expression only under a specific condition, it is unlikely that our study or any other attempt to categorize NTS neurons in a limited number of baseline conditions would detect that subpopulation.

Another limitation is that we deliberately focused on the NTS and not the area postrema, which contains neurons that detect toxins and evoke nausea, because neuronal subpopulations in the area postrema were described in a previous study (Zhang et al. 2021). Also, while we focused on transcription factors, neuropeptides, and a limited number of other genes, additional gene-families may be useful for distinguishing NTS neurons. In particular, G-protein–coupled receptors can be useful targets for drug therapies, and we and others have identified interesting expression patterns for a handful of G-protein–coupled receptors, including the angiotensin II receptor *Agtr1a* and the secretin receptor *Sctr* in the medial NTS (Gasparini et al. 2019; Gonzalez et al. 2012; Y. Liu et al. 2023; Resch et al. 2017), as well as *Calcr*, *Gfral*, and *Glp1r* the area postrema (W. Cheng, Gonzalez, et al. 2020; W. Cheng et al. 2021; Huang et al. 2024; Ludwig et al. 2021; Qiu et al. 2023; Zhang et al. 2021). These receptors may allow circulating peptide hormones and drugs to modulate the activity of specific subsets of neurons in the subpostremal NTS and area postrema (Resch et al. 2017; Zhang et al. 2021).

In addition, we focused on glutamatergic NTS neurons without identifying subtype-specific markers for GABAergic neurons in this region. Most GABAergic neurons in the NTS probably function as local interneurons, without long-range axonal projections outside the NTS, but some may project axons to the ventrolateral medulla and other sites, and these projection neurons likely include the large GABAergic "pump cells" in the ventrolateral NTS, which control the pulmonary Hering–Breuer reflex (Tanaka and Ezure 2004). The developmental lineage of these and other GABAergic neurons in the NTS remains unknown, but it is presumably different from that of *Lmx1b*- and *Phox2b*-lineage glutamatergic neurons. Further work is needed to determine this lineage and whether this region includes functionally distinct GABAergic subpopulations demarcated by specific genetic markers.

Finally, beyond the core ontology of *Lmx1b* and *Phox2b* expression, our approach focused on subpopulation boundaries demarcated by mutually exclusive, single gene expression. This approach successfully distinguished NTS subpopulations expressing *Gcg*, *Grp*, HSD2/*Hsd11b2*, *Npff*, *Pou3f1/Nos1*, and TH/*Slc6a2*, but some subpopulations may not express a single, unique marker. Isolating those subpopulations will require multidimensional analysis. Depending on the chosen algorithm and other analytic design choices, clustering multidimensional data from many thousands or millions of single-cell transcriptomes can generate divergent results, even from the same dataset, and previous scRNA-seq studies have reported several different neuronal clustering schemas (Dowsett et al. 2021; Ilanges et al. 2022; Lowenstein et al. 2023; Ludwig et al. 2021; Reiner et al. 2022; Su et al. 2024; Tao et al. 2021; Zhang et al. 2021). Future work using spatial transcriptomic methods (K. H. Chen et al. 2015) will extend our present findings and help clarify discrepancies among previous scRNA-seq reports. Regardless of the analytic methods used, combined labeling of individual genes and proteins in brain tissue remains the gold-standard way to confirm or refute any newly hypothesized molecular demarcations derived from algorithmic cluster analysis.

4.4 | Conclusion

Our study provides a useful framework for targeting specific subpopulations of NTS neurons. Future work in this region should add scaffolding to this curated foundation of molecular markers, which will help guide translational work in other species, including humans.

Author Contributions

J.C.G. planned the project, secured funding, and drafted the manuscript with S.G. S.G., G.A.P., and A.S.P.M. performed histology and microscopy. S.G. and G.A.P. performed high-sensitivity in situ hybridization. G.A.P. and S.G. drafted the figures. G.A.P., S.G., and J.C.G. edited the figures and figure legends together. S.G. and J.C.G. edited and finalized the text together. All authors approved the text and figures in this manuscript.

Conflicts of Interest

The authors declare no conflicts of interest.

Data Availability Statement

The data that support the findings of this study are available from the corresponding author upon reasonable request.

Peer Review

The peer review history for this article is available at https://publons.com/publon/10.1002/cne.70004.

References

Aklan, I., N. Sayar Atasoy, Y. Yavuz, et al. 2020. "NTS Catecholamine Neurons Mediate Hypoglycemic Hunger via Medial Hypothalamic Feeding Pathways." *Cell Metabolism* 31, no. 2: 313–326. e5. https://doi.org/10.1016/j.cmet.2019.11.016.

Altschuler, S. M., X. M. Bao, D. Bieger, D. A. Hopkins, and R. R. Miselis. 1989. "Viscerotopic Representation of the Upper Alimentary Tract in the Rat: Sensory Ganglia and Nuclei of the Solitary and Spinal Trigeminal Tracts." *Journal of Comparative Neurology* 283, no. 2: 248–268. https://doi.org/10.1002/cne.902830207.

Armstrong, D. M., V. M. Pickel, T. H. Joh, D. J. Reis, and R. J. Miller. 1981. "Immunocytochemical Localization of Catecholamine Synthesizing Enzymes and Neuropeptides in Area Postrema and Medial Nucleus Tractus Solitarius of Rat Brain." *Journal of Comparative Neurology* 196, no. 3: 505–517. https://doi.org/10.1002/cne.901960312.

Bassi, J. K., A. A. Connelly, A. G. Butler, et al. 2022. "Analysis of the Distribution of Vagal Afferent Projections From Different Peripheral Organs to the Nucleus of the Solitary Tract in Rats." *Journal of Comparative Neurology* 530, no. 17: 3072–3103. https://doi.org/10.1002/cne.25398.

Beckstead, R. M., J. R. Morse, and R. Norgren. 1980. "The Nucleus of the Solitary Tract in the Monkey: Projections to the Thalamus and Brain Stem Nuclei." *Journal of Comparative Neurology* 190, no. 2: 259–282. https://doi.org/10.1002/cne.901900205.

Chen, K. H., A. N. Boettiger, J. R. Moffitt, S. Wang, and X. Zhuang. 2015. "RNA Imaging. Spatially Resolved, Highly Multiplexed RNA Profiling in Single Cells." *Science* 348, no. 6233: aaa6090. https://doi.org/10.1126/science.aaa6090.

Chen, J., M. Cheng, L. Wang, et al. 2020. "A Vagal-NTS Neural Pathway That Stimulates Feeding." *Current Biology* 30, no. 20: 3986–3998. e3985. https://doi.org/10.1016/j.cub.2020.07.084.

Chen, C., S. L. Dun, N. J. Dun, and J. K. Chang. 1999. "Prolactin-Releasing Peptide-Immunoreactivity in A1 and A2 Noradrenergic Neurons of the Rat Medulla." *Brain Research* 822, no. 1–2: 276–279. https://doi.org/10.1016/s0006-8993(99)01153-1.

Cheng, L., A. Arata, R. Mizuguchi, et al. 2004. "Tlx3 and Tlx1 Are Post-Mitotic Selector Genes Determining Glutamatergic Over GABAergic Cell Fates." *Nature Neuroscience* 7, no. 5: 510–517. https://doi.org/10.1038/nn1221.

Cheng, W., I. Gonzalez, W. Pan, et al. 2020. "Calcitonin Receptor Neurons in the Mouse Nucleus Tractus Solitarius Control Energy Balance via the Non-Aversive Suppression of Feeding." *Cell Metabolism* 31, no. 2: 301–312. e5. https://doi.org/10.1016/j.cmet.2019.12.012.

Cheng, W., E. Ndoka, C. Hutch, et al. 2020. "Leptin Receptor-Expressing Nucleus Tractus Solitarius Neurons Suppress Food Intake Independently of GLP1 in Mice." *JCI Insight* 5, no. 7: e134359. https://doi.org/10.1172/jci.insight.134359.

Cheng, W., E. Ndoka, J. N. Maung, et al. 2021. "NTS Prlh Overcomes Orexigenic Stimuli and Ameliorates Dietary and Genetic Forms of Obesity." *Nature Communications* 12, no. 1: 5175. https://doi.org/10.1038/s41467-021-25525-3.

Cheng, L., O. A. Samad, Y. Xu, et al. 2005. "Lbx1 and Tlx3 Are Opposing Switches in Determining GABAergic Versus Glutamatergic Transmitter Phenotypes." *Nature Neuroscience* 8, no. 11: 1510–1515. https://doi.org/10.1038/nn1569.

Contreras, R. J., R. M. Beckstead, and R. Norgren. 1982. "The Central Projections of the Trigeminal, Facial, Glossopharyngeal and Vagus Nerves: An Autoradiographic Study in the Rat." *Journal of the Autonomic Nervous System* 6, no. 3: 303–322. https://doi.org/10.1016/0165-1838(82)90003-0.

Cui, K., Y. Xia, A. Patnaik, et al. 2024. "Genetic Identification of Medullary Neurons Underlying Congenital Hypoventilation." *Science Advances* 10, no. 25: eadj0720. https://doi.org/10.1126/sciadv.adj0720.

Cunningham, E. T. Jr., and P. E. Sawchenko. 1989. "A Circumscribed Projection From the Nucleus of the Solitary Tract to the Nucleus Ambiguus

in the Rat: Anatomical Evidence for Somatostatin-28-immunoreactive Interneurons Subserving Reflex Control of Esophageal Motility." *Journal of Neuroscience* 9, no. 5: 1668–1682.

Cutsforth-Gregory, J. K., and E. E. Benarroch. 2017. "Nucleus of the Solitary Tract, Medullary Reflexes, and Clinical Implications." *Neurology* 88, no. 12: 1187–1196. https://doi.org/10.1212/WNL.0000000000003751.

Dai, J. X., Z. L. Hu, M. Shi, C. Guo, and Y. Q. Ding. 2008. "Postnatal Ontogeny of the Transcription Factor Lmx1b in the Mouse Central Nervous System." *Journal of Comparative Neurology* 509, no. 4: 341–355. https://doi.org/10.1002/cne.21759.

Dauger, S., A. Pattyn, F. Lofaso, et al. 2003. "Phox2b Controls the Development of Peripheral Chemoreceptors and Afferent Visceral Pathways." *Development* 130, no. 26: 6635–6642. https://doi.org/10.1242/dev.00866.

Ding, Y. Q., U. Marklund, W. Yuan, et al. 2003. "Lmx1b Is Essential for the Development of Serotonergic Neurons." *Nature Neuroscience* 6, no. 9: 933–938. https://doi.org/10.1038/nn1104.

Dowsett, G. K. C., B. Y. H. Lam, J. A. Tadross, et al. 2021. "A Survey of the Mouse Hindbrain in the Fed and Fasted States Using Single-Nucleus RNA Sequencing." *Molecular Metabolism* 53: 101240. https://doi.org/10.1016/j.molmet.2021.101240.

Ezure, K., and I. Tanaka. 2004. "GABA, in Some Cases Together With Glycine, Is Used as the Inhibitory Transmitter by Pump Cells in the Hering-Breuer Reflex Pathway of the Rat." *Neuroscience* 127, no. 2: 409–417. https://doi.org/10.1016/j.neuroscience.2004.05.032.

Ganchrow, D., J. R. Ganchrow, V. Cicchini, et al. 2014. "Nucleus of the Solitary Tract in the C57BL/6J Mouse: Subnuclear Parcellation, Chorda Tympani Nerve Projections, and Brainstem Connections." *Journal of Comparative Neurology* 522, no. 7: 1565–1596. https://doi.org/10.1002/cne.23484.

Gannot, N., X. Li, C. D. Phillips, et al. 2024. "A Vagal-Brainstem Interoceptive Circuit for Cough-Like Defensive Behaviors in Mice." *Nature Neuroscience* 27, no. 9: 1734–1744. https://doi.org/10.1038/s41593-024-01712-5.

Gasparini, S., J. M. Howland, A. J. Thatcher, and J. C. Geerling. 2020. "Central Afferents to the Nucleus of the Solitary Tract in Rats and Mice." *Journal of Comparative Neurology* 528, no. 16: 2708–2728. https://doi.org/10.1002/cne.24927.

Gasparini, S., M. R. Melo, G. M. F. Andrade-Franze, J. C. Geerling, J. V. Menani, and E. Colombari. 2018. "Aldosterone Infusion Into the 4(th) Ventricle Produces Sodium Appetite With Baroreflex Attenuation Independent of Renal or Blood Pressure Changes." *Brain Research* 1698: 70–80. https://doi.org/10.1016/j.brainres.2018.06.023.

Gasparini, S., L. Peltekian, M. C. McDonough, et al. 2024. "Aldosterone-induced Salt Appetite Requires HSD2 Neurons." *JCI Insight* e175087. https://doi.org/10.1172/jci.insight.175087.

Gasparini, S., J. M. Resch, S. V. Narayan, et al. 2019. "Aldosterone-sensitive HSD2 Neurons in Mice." *Brain Structure and Function* 224, no. 1: 387–417. https://doi.org/10.1007/s00429-018-1778-y.

Gaykema, R. P., B. A. Newmyer, M. Ottolini, et al. 2017. "Activation of Murine Pre-Proglucagon-Producing Neurons Reduces Food Intake and Body Weight." *Journal of Clinical Investigation* 127, no. 3: 1031–1045. https://doi.org/10.1172/JCI81335.

Geerling, J. C., P. C. Chimenti, and A. D. Loewy. 2008. "Phox2b Expression in the Aldosterone-Sensitive HSD2 Neurons of the NTS." *Brain Research* 1226: 82–88. https://doi.org/10.1016/j.brainres.2008.05.072.

Geerling, J. C., M. Kawata, and A. D. Loewy. 2006. "Aldosterone-Sensitive Neurons in the Rat Central Nervous System." *Journal of Comparative Neurology* 494, no. 3: 515–527. https://doi.org/10.1002/cne.20808.

Geerling, J. C., and A. D. Loewy. 2006. "Aldosterone-Sensitive Neurons in the Nucleus of the Solitary Tract: Efferent Projections." *Journal of Comparative Neurology* 497, no. 2: 223–250. https://doi.org/10.1002/cne.20993.

Gonzalez, A. D., G. Wang, E. M. Waters, et al. 2012. "Distribution of Angiotensin Type 1a Receptor-Containing Cells in the Brains of Bacterial Artificial Chromosome Transgenic Mice." *Neuroscience* 226: 489–509. https://doi.org/10.1016/j.neuroscience.2012.08.039.

Gray, P. A. 2013. "Transcription Factors Define the Neuroanatomical Organization of the Medullary Reticular Formation." *Frontiers in Neuroanatomy* 7: 7. https://doi.org/10.3389/fnana.2013.00007.

Guo, C., H. Y. Qiu, M. Shi, et al. 2008. "Lmx1b-Controlled Isthmic Organizer Is Essential for Development of Midbrain Dopaminergic Neurons." *Journal of Neuroscience* 28, no. 52: 14097–14106. https://doi.org/10.1523/JNEUROSCI.3267-08.2008.

Hamilton, R. B., and R. Norgren. 1984. "Central Projections of Gustatory Nerves in the Rat." *Journal of Comparative Neurology* 222, no. 4: 560–577. https://doi.org/10.1002/cne.902220408.

Herbert, H., M. M. Moga, and C. B. Saper. 1990. "Connections of the Parabrachial Nucleus With the Nucleus of the Solitary Tract and the Medullary Reticular Formation in the Rat." *Journal of Comparative Neurology* 293, no. 4: 540–580.

Herbert, H., and C. B. Saper. 1990. "Cholecystokinin-, Galanin-, and Corticotropin-Releasing Factor-Like Immunoreactive Projections From the Nucleus of the Solitary Tract to the Parabrachial Nucleus in the Rat." *Journal of Comparative Neurology* 293, no. 4: 581–598. https://doi.org/10.1002/cne.902930405.

Hernandez-Miranda, L. R., D. M. Ibrahim, P. L. Ruffault, et al. 2018. "Mutation in LBX1/Lbx1 Precludes Transcription Factor Cooperativity and Causes Congenital Hypoventilation in Humans and Mice." *PNAS* 115, no. 51: 13021–13026. https://doi.org/10.1073/pnas.1813520115.

Hernandez-Miranda, L. R., T. Müller, and C. Birchmeier. 2017. "The Dorsal Spinal Cord and Hindbrain: from Developmental Mechanisms to Functional Circuits." *Developmental Biology* 432, no. 1: 34–42. https://doi.org/10.1016/j.ydbio.2016.10.008.

Hirsch, D., A. Kohl, Y. Wang, and D. Sela-Donenfeld. 2021. "Axonal Projection Patterns of the Dorsal Interneuron Populations in the Embryonic Hindbrain." *Frontiers in Neuroanatomy* 15, no. 112: 793161. https://doi.org/10.3389/fnana.2021.793161.

Holt, M. K. 2022. "The Ins and Outs of the Caudal Nucleus of the Solitary Tract: An Overview of Cellular Populations and Anatomical Connections." *Journal of Neuroendocrinology* 34, no. 6: e13132. https://doi.org/10.1111/jne.13132.

Holt, M. K., L. E. Pomeranz, K. T. Beier, F. Reimann, F. M. Gribble, and L. Rinaman. 2019. "Synaptic Inputs to the Mouse Dorsal Vagal Complex and Its Resident Preproglucagon Neurons." *Journal of Neuroscience* 39, no. 49: 9767–9781. https://doi.org/10.1523/JNEUROSCI.2145-19.2019.

Holt, M. K., J. E. Richards, D. R. Cook, et al. 2019. "Preproglucagon Neurons in the Nucleus of the Solitary Tract Are the Main Source of Brain GLP-1, Mediate Stress-Induced Hypophagia, and Limit Unusually Large Intakes of Food." *Diabetes* 68, no. 1: 21–33. https://doi.org/10.2337/db18-0729.

Holt, M. K., and L. Rinaman. 2022. "The Role of Nucleus of the Solitary Tract Glucagon-Like Peptide-1 and Prolactin-Releasing Peptide Neurons in Stress: Anatomy, Physiology and Cellular Interactions." *British Journal of Pharmacology* 179, no. 4: 642–658. https://doi.org/10.1111/bph.15576.

Huang, K. P., A. A. Acosta, M. Y. Ghidewon, et al. 2024. "Dissociable Hindbrain GLP1R Circuits for Satiety and Aversion." *Nature* 632, no. 8025: 585–593. https://doi.org/10.1038/s41586-024-07685-6.

Huo, L., Z. Ye, M. Liu, et al. 2024. "Brain Circuits for Retching-Like Behavior." *National Science Review* 11, no. 1: nwad256. https://doi.org/10.1093/nsr/nwad256.

Ilanges, A., R. Shiao, J. Shaked, J. D. Luo, X. Yu, and J. M. Friedman. 2022. "Brainstem ADCYAP1(+) Neurons Control Multiple Aspects of Sickness Behaviour." *Nature* 609, no. 7928: 761–771. https://doi.org/10.1038/s41586-022-05161-7.

Jarvie, B. C., and R. D. Palmiter. 2017. "HSD2 Neurons in the Hindbrain Drive Sodium Appetite." *Nature Neuroscience* 20, no. 2: 167–169. https://doi.org/10.1038/nn.4451.

Kalia, M., and J. M. Sullivan. 1982. "Brainstem Projections of Sensory and Motor Components of the Vagus Nerve in the Rat." *Journal of Comparative Neurology* 211, no. 3: 248–265. https://doi.org/10.1002/cne.902110304.

Kang, B. J., D. A. Chang, D. D. Mackay, et al. 2007. "Central Nervous System Distribution of the Transcription Factor Phox2b in the Adult Rat." *Journal of Comparative Neurology* 503, no. 5: 627–641. https://doi.org/10.1002/cne.21409.

Karthik, S., D. Huang, Y. Delgado, et al. 2022. "Molecular Ontology of the Parabrachial Nucleus." *Journal of Comparative Neurology* 530, no. 10: 1658–1699. https://doi.org/10.1002/cne.25307.

Kivipelto, L. 1991. "Ultrastructural Localization of Neuropeptide FF, a New Neuropeptide in the Brain and Pituitary of Rats." *Regulatory Peptides* 34, no. 3: 211–224. https://doi.org/10.1016/0167-0115(91)90180-o.

Kreisler, A. D., and L. Rinaman. 2016. "Hindbrain Glucagon-Like Peptide-1 Neurons Track Intake Volume and Contribute to Injection Stress-Induced Hypophagia in Meal-Entrained Rats." *American Journal of Physiology. Regulatory, Integrative and Comparative Physiology* 310, no. 10: R906–916. https://doi.org/10.1152/ajpregu.00243.2015.

Liu, Y., J. A. Wei, Z. Luo, et al. 2023. "A Gut-Brain Axis Mediates Sodium Appetite via Gastrointestinal Peptide Regulation on a Medulla-Hypothalamic Circuit." *Science Advances* 9, no. 7: eadd5330. https://doi.org/10.1126/sciadv.add5330.

Liu, Z. R., M. Shi, Z. L. Hu, et al. 2010. "A Refined Map of Early Gene Expression in the Dorsal Rhombomere 1 of Mouse Embryos." *Brain Research Bulletin* 82, no. 1-2: 74–82. https://doi.org/10.1016/j.brainresbull.2010.02.010.

Loewy, A. D., and H. Burton. 1978. "Nuclei of the Solitary Tract: Efferent Projections to the Lower Brain Stem and Spinal Cord of the Cat." *Journal of Comparative Neurology* 181, no. 2: 421–449. https://doi.org/10.1002/cne.901810211.

Lowenstein, E. D., P. L. Ruffault, A. Misios, et al. 2023. "Prox2 and Runx3 Vagal Sensory Neurons Regulate Esophageal Motility." *Neuron* 111, no. 14: 2184–2200. e2187. https://doi.org/10.1016/j.neuron.2023.04.025.

Ludwig, M. Q., W. Cheng, D. Gordian, et al. 2021. "A Genetic Map of the Mouse Dorsal Vagal Complex and Its Role in Obesity." *Nature Metabolism* 3, no. 4: 530–545. https://doi.org/10.1038/s42255-021-00363-1.

Ly, T., J. Y. Oh, N. Sivakumar, et al. 2023. "Sequential Appetite Suppression by Oral and Visceral Feedback to the Brainstem." *Nature* 624, no. 7990: 130–137. https://doi.org/10.1038/s41586-023-06758-2.

McRitchie, D. A., and I. Tork. 1993. "The Internal Organization of the Human Solitary Nucleus." *Brain Research Bulletin* 31, no. 1-2: 171–193. https://doi.org/10.1016/0361-9230(93)90024-6.

Miller, R. L., M. M. Knuepfer, M. H. Wang, G. O. Denny, P. A. Gray, and A. D. Loewy. 2012. "Fos-Activation of FoxP2 and Lmx1b Neurons in the Parabrachial Nucleus Evoked by Hypotension and Hypertension in Conscious Rats." *Neuroscience* 218: 110–125. https://doi.org/10.1016/j.neuroscience.2012.05.049.

Pattyn, A., C. Goridis, and J. F. Brunet. 2000. "Specification of the Central Noradrenergic Phenotype by the Homeobox Gene Phox2b." *Molecular and Cellular Neuroscience* 15, no. 3: 235–243. https://doi.org/10.1006/mcne.1999.0826.

Pattyn, A., M. Hirsch, C. Goridis, and J. F. Brunet. 2000. "Control of Hindbrain Motor Neuron Differentiation by the Homeobox Gene Phox2b." *Development* 127, no. 7: 1349–1358.

Pattyn, A., X. Morin, H. Cremer, C. Goridis, and J. F. Brunet. 1999. "The Homeobox Gene Phox2b Is Essential for the Development of Autonomic Neural Crest Derivatives." *Nature* 399, no. 6734: 366–370. https://doi.org/10.1038/20700.

Pauli, J. L., J. Y. Chen, M. L. Basiri, et al. 2022. "Molecular and Anatomical Characterization of Parabrachial Neurons and Their Axonal Projections." *Elife* 11: e81868. https://doi.org/10.7554/eLife.81868.

Qian, Y., B. Fritzsch, S. Shirasawa, C. L. Chen, Y. Choi, and Q. Ma. 2001. "Formation of Brainstem (nor)Adrenergic Centers and First-Order Relay Visceral Sensory Neurons Is Dependent on Homeodomain Protein Rnx/Tlx3." *Genes & Development* 15, no. 19: 2533–2545. https://doi.org/10.1101/gad.921501.

Qiu, W., C. R. Hutch, Y. Wang, et al. 2023. "Multiple NTS Neuron Populations Cumulatively Suppress Food Intake." *Elife* 12: e85640. https://doi.org/10.7554/eLife.85640.

Quillet, R., A. C. Dickie, E. Polgar, et al. 2023. "Characterisation of NPFF-Expressing Neurons in the Superficial Dorsal Horn of the Mouse Spinal Cord." *Scientific Reports* 13, no. 1: 5891. https://doi.org/10.1038/s41598-023-32720-3.

Ran, C., J. C. Boettcher, J. A. Kaye, C. E. Gallori, and S. D. Liberles. 2022. "A Brainstem Map for Visceral Sensations." *Nature* 609, no. 7926: 320–326. https://doi.org/10.1038/s41586-022-05139-5.

Reiner, B. C., R. C. Crist, T. Borner, R. P. Doyle, M. R. Hayes, and B. C. De Jonghe. 2022. "Single Nuclei RNA Sequencing of the Rat AP and NTS Following GDF15 Treatment." *Molecular Metabolism* 56: 101422. https://doi.org/10.1016/j.molmet.2021.101422.

Resch, J. M., H. Fenselau, J. C. Madara, et al. 2017. "Aldosterone-Sensing Neurons in the NTS Exhibit State-Dependent Pacemaker Activity and Drive Sodium Appetite via Synergy With Angiotensin II Signaling." *Neuron* 96, no. 1: 190–206. e197. https://doi.org/10.1016/j.neuron.2017.09.014.

Riche, D., J. De Pommery, and D. Menetrey. 1990. "Neuropeptides and Catecholamines in Efferent Projections of the Nuclei of the Solitary Tract in the Rat." *Journal of Comparative Neurology* 293, no. 3: 399–424. https://doi.org/10.1002/cne.902930306.

Rinaman, L. 2010. "Ascending Projections From the Caudal Visceral Nucleus of the Solitary Tract to Brain Regions Involved in Food Intake and Energy Expenditure." *Brain Research* 1350: 18–34. https://doi.org/10.1016/j.brainres.2010.03.059.

Roman, C. W., S. R. Sloat, and R. D. Palmiter. 2017. "A Tale of Two Circuits: CCK(NTS) Neuron Stimulation Controls Appetite and Induces Opposing Motivational States by Projections to Distinct Brain Regions." *Neuroscience* 358: 316–324. https://doi.org/10.1016/j.neuroscience.2017.06.049.

Sayar-Atasoy, N., C. Laule, I. Aklan, et al. 2023. "Adrenergic Modulation of Melanocortin Pathway by Hunger Signals." *Nature Communications* 14, no. 1: 6602. https://doi.org/10.1038/s41467-023-42362-8.

Scott, M. M., K. W. Williams, J. Rossi, C. E. Lee, and J. K. Elmquist. 2011. "Leptin Receptor Expression in Hindbrain Glp-1 Neurons Regulates Food Intake and Energy Balance in Mice." *Journal of Clinical Investigation* 121, no. 6: 2413–2421. https://doi.org/10.1172/JCI43703.

Siletti, K., R. Hodge, A. Mossi Albiach, et al. 2023. "Transcriptomic Diversity of Cell Types Across the Adult Human Brain." *Science* 382, no. 6667: eadd7046. https://doi.org/10.1126/science.add7046.

Smidt, M. P., C. H. Asbreuk, J. J. Cox, H. Chen, R. L. Johnson, and J. P. Burbach. 2000. "A Second Independent Pathway for Development of Mesencephalic Dopaminergic Neurons Requires Lmx1b." *Nature Neuroscience* 3, no. 4: 337–341. https://doi.org/10.1038/73902.

Stornetta, R. L., T. S. Moreira, A. C. Takakura, et al. 2006. "Expression of Phox2b by Brainstem Neurons Involved in Chemosensory Integration in the Adult Rat." *Journal of Neuroscience* 26, no. 40: 10305–10314. https://doi.org/10.1523/JNEUROSCI.2917-06.2006.

Stornetta, R. L., C. P. Sevigny, and P. G. Guyenet. 2002. "Vesicular Glutamate Transporter DNPI/VGLUT2 mRNA Is Present in C1 and Several Other Groups of Brainstem Catecholaminergic Neurons." *Journal of Comparative Neurology* 444, no. 3: 191–206. https://doi.org/10.1002/cne.10141.

Su, Y., J. Xu, Z. Zhu, et al. 2024. "Brainstem Dbh(+) Neurons Control Allergen-Induced Airway Hyperreactivity." *Nature* 631, no. 8021: 601–609. https://doi.org/10.1038/s41586-024-07608-5.

Szabo, N. E., R. V. da Silva, S. G. Sotocinal, H. U. Zeilhofer, J. S. Mogil, and A. Kania. 2015. "Hoxb8 intersection Defines a Role for Lmx1b in Excitatory Dorsal Horn Neuron Development, Spinofugal Connectivity, and Nociception." *Journal of Neuroscience* 35, no. 13: 5233–5246. https://doi.org/10.1523/JNEUROSCI.4690-14.2015.

Tanaka, I., and K. Ezure. 2004. "Overall Distribution of GLYT2 mRNA-Containing Versus GAD67 mRNA-Containing Neurons and Colocalization of Both mRNAs in Midbrain, Pons, and Cerebellum in Rats." *Neuroscience Research* 49, no. 2: 165–178. https://doi.org/10.1016/j.neures.2004.02.007.

Tao, J., J. N. Campbell, L. T. Tsai, C. Wu, S. D. Liberles, and B. B. Lowell. 2021. "Highly Selective Brain-to-Gut Communication via Genetically Defined Vagus Neurons." *Neuron* 109, no. 13: 2106–2115. e4. https://doi.org/10.1016/j.neuron.2021.05.004.

Ter Horst, G. J., P. de Boer, P. G. Luiten, and J. D. van Willigen. 1989. "Ascending Projections From the Solitary Tract Nucleus to the Hypothalamus. A Phaseolus Vulgaris Lectin Tracing Study in the Rat." *Neuroscience* 31, no. 3: 785–797.

van der Kooy, D., L. Y. Koda, J. F. McGinty, C. R. Gerfen, and F. E. Bloom. 1984. "The Organization of Projections From the Cortex, Amygdala, and Hypothalamus to the Nucleus of the Solitary Tract in Rat." *Journal of Comparative Neurology* 224, no. 1: 1–24. https://doi.org/10.1002/cne.902240102.

Vrang, N., C. B. Phifer, M. M. Corkern, and H. R. Berthoud. 2003. "Gastric Distension Induces c-Fos in Medullary GLP-1/2-Containing Neurons." *American Journal of Physiology. Regulatory, Integrative and Comparative Physiology* 285, no. 2: R470–R478. https://doi.org/10.1152/ajpregu.00732.2002.

Wang, X. F., J. J. Liu, J. Xia, J. Liu, V. Mirabella, and Z. P. Pang. 2015. "Endogenous Glucagon-Like Peptide-1 Suppresses High-Fat Food Intake by Reducing Synaptic Drive Onto Mesolimbic Dopamine Neurons." *Cell Reports* 12, no. 5: 726–733. https://doi.org/10.1016/j.celrep.2015.06.062.

Whitehead, M. C. 1988. "Neuronal Architecture of the Nucleus of the Solitary Tract in the Hamster." *Journal of Comparative Neurology* 276, no. 4: 547–572. https://doi.org/10.1002/cne.902760409.

Whitehead, M. C., A. Bergula, and K. Holliday. 2000. "Forebrain Projections to the Rostral Nucleus of the Solitary Tract in the Hamster." *Journal of Comparative Neurology* 422, no. 3: 429–447.

Wiedner, E. B., X. Bao, and S. M. Altschuler. 1995. "Localization of Nitric Oxide Synthase in the Brain Stem Neural Circuit Controlling Esophageal Peristalsis in Rats." *Gastroenterology* 108, no. 2: 367–375. https://doi.org/10.1016/0016-5085(95)90062-4.

Xiang, C. X., K. H. Zhang, R. L. Johnson, M. F. Jacquin, and Z. F. Chen. 2012. "The Transcription Factor, Lmx1b, Promotes a Neuronal Glutamate Phenotype and Suppresses a GABA One in the Embryonic Trigeminal Brainstem Complex." *Somatosensory & Motor Research* 29, no. 1: 1–12. https://doi.org/10.3109/08990220.2011.650869.

Yamazoe, M., S. Shiosaka, T. Shibasaki, et al. 1984. "Distribution of Six Neuropeptides in the Nucleus Tractus Solitarii of the Rat: An Immunohistochemical Analysis." *Neuroscience* 13, no. 4: 1243–1266. https://doi.org/10.1016/0306-4522(84)90296-3.

Yao, Z., C. T. J. van Velthoven, M. Kunst, et al. 2023. "A High-Resolution Transcriptomic and Spatial Atlas of Cell Types in the Whole Mouse Brain." *Nature* 624, no. 7991: 317–332. https://doi.org/10.1038/s41586-023-06812-z.

Zeisel, A., H. Hochgerner, P. Lonnerberg, et al. 2018. "Molecular Architecture of the Mouse Nervous System." *Cell* 174, no. 4: 999–1014. e1022. https://doi.org/10.1016/j.cell.2018.06.021.

Zhang, C., J. A. Kaye, Z. Cai, Y. Wang, S. L. Prescott, and S. D. Liberles. 2021. "Area Postrema Cell Types That Mediate Nausea-Associated Behaviors." *Neuron* 109, no. 3: 461–472. e465. https://doi.org/10.1016/j.neuron.2020.11.010.

Zhao, Z. Q., M. Scott, S. Chiechio, et al. 2006. "Lmx1b Is Required for Maintenance of Central Serotonergic Neurons and Mice Lacking Central Serotonergic System Exhibit Normal Locomotor Activity." *Journal of Neuroscience* 26, no. 49: 12781–12788. https://doi.org/10.1523/JNEUROSCI.4143-06.2006.

Zheng, H., R. L. Stornetta, K. Agassandian, and L. Rinaman. 2015. "Glutamatergic Phenotype of Glucagon-Like Peptide 1 Neurons in the Caudal Nucleus of the Solitary Tract in Rats." *Brain Structure & Function* 220, no. 5: 3011–3022. https://doi.org/10.1007/s00429-014-0841-6.